

What can geophysical geoarchaeology reveal about the archaeology and depositional history of the site of Klein Hoek 1, South Africa?

Oliver Hatswell

04/11/2021



A thesis submitted in fulfilment of the requirements of the degree of Master of
Archaeology and Heritage Management, College of Humanities, Arts and
Social Sciences, Flinders University of South Australia

Table of Contents

List of Figures	iii
List of Tables.....	iv
Abstract.....	v
Declaration of Candidate.....	vii
Acknowledgements.....	viii
1 Introduction	1
1.1 Research Question	2
1.2 Thesis Outline	3
2 Study Area.....	5
3 Literature Review.....	10
3.1 The Technocomplexes	11
3.2 Rock Shelters vs Open-Air Sites.....	14
3.3 Archaeology in the Doring River Catchment.....	17
3.4 Geophysics in South Africa.....	23
3.5 Summary.....	25
4 Methods.....	27
4.1 Topographic Survey	27
4.2 Geological Mapping	27
4.3 Overview of Geophysical Techniques.....	28
4.4 Electrical Resistivity Tomography.....	30
4.5 Magnetometry	37
4.6 Magnetic Susceptibility	42
5 Results.....	48
5.1 Site Survey	48
5.2 Electrical Resistivity Tomography Results.....	50
5.2.1 Line 1	50
5.2.2 Line 2	53
5.2.3 Line 3	56
5.2.4 Summary	59
5.3 Magnetometer Results	60
5.4 Magnetic Susceptibility Results.....	61
5.4.1 Trench 1.....	61
5.4.2 Trench 5.....	63

5.4.3 Trench 6.....	64
5.4.4 Trench 10	65
5.4.5 Summary	66
6 Discussion.....	67
6.1 Electrical Resistivity Tomography.....	67
6.2 Magnetometry	72
6.3 Magnetic Susceptibility	74
6.4 Summary.....	75
7 Conclusion	78
7.1 The Geophysical Survey at KH1	78
7.2 Limitations	79
7.3 Future Research.....	81
References	83

List of Figures

Figure 1: Location of Klein Hoek 1. a) Archaeological survey area. b) Doring River Catchment and location of Klein Hoek 1 within it. c) Regional context of the Doring River catchment (Ames et al. 2020b:3).....	5
Figure 2: Oblique view of Klein Hoek 1 looking south, with a white line representing the border of the site and the location of the fence line, scree slope, basal cobble bed (point bar), and heuweltjies indicated (Ames et al. 2020b:4).	6
Figure 3: The artefacts and sediment bodies located across KH1. A) A selection of bifacial points from the Still Bay cluster. B) Engraved ochre (Shaw et al. 2019:415).	7
Figure 4: Photo of Klein Hoek 1, looking northeast, with the location of the stone tool cluster (Mackay et al. 2018:27).....	8
Figure 5: Map of significant late Pleistocene sites in southern Africa.....	10
Figure 6: Map of South Africa showing the location of the Doring River Archaeology Project study area. Circles = rock shelters. Squares = open-air sites. EB = Elands Bay, DPK = Diepkloof, KK = Klein Kliphuis, KFR = Klipfonteinrand, MRS = Mertenhof (Ames et al. 2020a:395).....	17
Figure 7: Western side of the test pit at PL1 with the location of OSL samples and proposed paleosol location (Mackay et al. 2014:48).	21
Figure 8: Site plan of KH1 showing the location of the geophysical survey.	30
Figure 9: The location of the ERT survey at KH1.	35
Figure 10: The magnetometry survey area.....	41
Figure 11: Trench 1.....	45
Figure 12: Trench 5.....	45
Figure 13: Trench 6.....	46
Figure 14: Trench 10.....	46
Figure 15: Location of the trenches where magnetic susceptibility tests were conducted.	47
Figure 16: Geological map of KH1.	49
Figure 17: The location of Line 1.....	50
Figure 18: Wenner array of Line 1.....	51
Figure 19: Dipole-dipole array of Line 1	52
Figure 20: The location of Line 2.....	53
Figure 21: Wenner array of Line 2.....	54
Figure 22: Dipole-dipole array of Line 2.	55
Figure 23: The location of Line 3.....	56
Figure 24: Wenner array of Line 3.....	57
Figure 25: Dipole-dipole array of Line 3.	58
Figure 26: Results of the 20 x 20 m magnetometry grids combined into one map. The number of each grid is referenced underneath.....	60
Figure 27: Magnetic susceptibility results from Trench 1 (left). The location of Trench 1 (right).	62
Figure 28: Magnetic susceptibility results from Trench 5 (left). The location of Trench 5 (right).	63
Figure 29: Magnetic susceptibility results from Trench 6 (left). The location of Trench 6 (right).	64
Figure 30: Magnetic susceptibility results from Trench 10 (left). The location of Trench 10 (right).	65
Figure 31: Interpretations of the stratigraphy of Line 1 (top), Line 2 (middle), and Line 3 (bottom) based on the ERT sections.	69
Figure 32: Examples of small, highly resistive anomalies in the dipole-dipole array of Line 1 (left), the dipole-dipole array of Line 2 (centre), and the Wenner array of Line 3 (right).	70
Figure 33: Areas of high archaeological potential identified from analysis of the magnetometry survey.....	73

List of Tables

Table 1: Technocomplexes of the Middle Stone Age.....	13
Table 2: Indicative resistivities of common rocks and soil materials (Saad et al. 2012:371). 32	
Table 3: Information on the trenches where magnetic susceptibility tests were conducted.. 44	
Table 4: Description of the geological units of KH1.	49

Abstract

The primary goal of this research project was to utilise geophysical techniques to further understand the stratigraphy and archaeology of Klein Hoek 1, an open-air site located immediately adjacent to the Doring River in southern Africa. This survey utilized three geophysical methods; electrical resistivity tomography, magnetometry, and magnetic susceptibility. The results of the electrical resistivity tomography survey showed that the stratigraphic unit where an important cluster of bifacial points is located extends throughout the subsurface of the rest of the site and is at least 8 metres thick. The magnetometry survey revealed evidence of hearth anomalies within the subsurface, which are interpreted as areas of archaeological potential due to a correlation between the bifacial cluster and prehistoric burning. Finally, the magnetic susceptibility test displayed evidence of a paleosol in the subsurface on the eastern side of the site.

Southern Africa is one of the most significant archaeological regions in the world due to it being one of the earliest locations of behaviourally modern humans. The bifacial cluster located on the surface of Klein Hoek 1 is one of the most important collections of bifacial points in southern Africa, as it has only recently surfaced and still maintains coherency. Southern African archaeology has a long history of focusing research on rock shelter sites at the expense of open-air sites. This is due to the lower informative return of time and costs open-air sites have due to their complicated stratigraphy and potential loss of integrity. However, rock shelters only represent limited points in the landscape and history, and thus this focus has created a perspective of southern African prehistory that does not include all the available information making it limited and biased.

The results of this geophysical survey will primarily assist in future study and excavation of Klein Hoek 1. The ERT survey will provide a greater understanding of the stratigraphy of the site, while the magnetic susceptibility survey will locate any paleosols within the stratigraphy. Meanwhile, the magnetometry survey will identify any hearths within the subsurface and locate the areas of archaeological potential for future excavations. The success of this survey also demonstrates that geophysical methods are effective in a southern African open-air context. The further utilisation of geophysics in southern African archaeology could be invaluable in identifying the high archaeologically potential points of open-air sites making the study of these sites more time and cost-effective.

Declaration of Candidate

I certify that this thesis does not incorporate without acknowledgment any material previously submitted for a degree or diploma in any university; and that to the best of my knowledge and belief it does not contain any material previously published or written by another person except where due reference is made in the text.

Signature: Oliver Hatswell

Date: 4 November 2021

Acknowledgements

First, I would like to thank my supervisors Dr Ian Moffat and Dr Alexander Mackay.

Dr Ian Moffat introduced me to the wonderful world of geophysics and Dr Alexander Mackay taught me so much about southern African archaeology. Without their support and guidance, I would not have accomplished this paper.

Thanks to Associate Professor Brian Jones for his assistance in the field.

Thanks to Natasha Phillips for supplying me with papers for my literature review.

Finally, many thanks to my family, friends, and partner, for all their support and encouragement.

1 Introduction

Klein Hoek 1 (KH1), a Middle Stone Age open-air site located within the Doring River Catchment of South Africa, contains one of the most significant bifacial point collections in the region. These bifacial points are stone artefacts where both sides have been flaked and they are significant as they are attributed to the Still Bay industry which is associated with a range of distinctive behaviours associated with modern humans (Archer et al. 2016:58; Wadley 2015). The bifacial scatter found here is unique in that the collection has surfaced recently and has not been significantly eroded (Ames et al. 2020b:13; Shaw et al. 2019:414). Archaeological research on the Middle Stone Age in this region has traditionally been dominated by a focus on rock shelters due to limited research funds and the fact that rock shelters usually provide a greater return on time and costs (Fuchs et al. 2008: 425; Phillips et al. 2019:5852; Shaw et al. 2019:401). The problem with this approach is that rock shelter sites are geographically limited points in the landscape and thus, likely do not represent the full range of prehistoric human activities (Fuchs et al. 2008:426; Phillips et al. 2019:5853; Shaw et al. 2019:401). This has created a perspective of the MSA in southern Africa that due to its bias towards rock shelter archaeology, is limited and potentially incorrect.

A solution to the costly and timely study of open-air sites within the region may be the further application of geophysical surveys, which have been utilised to a very limited extent within southern African archaeology. This research project will perform a geophysical survey on KH1 to assist in the study of the site and other open-air sites within the wider Doring River catchment. The survey consisted of three parts, an electrical resistivity tomography (ERT) survey, a magnetometry survey, and a series of magnetic susceptibility tests. The project will assess the effectiveness of

these techniques in an open-air southern African context. If the geophysical methods prove to be successful, then the data will provide a unique snapshot of the stratigraphy of the catchment and demonstrate the use of geophysical techniques in open-air contexts.

1.1 Research Question

The primary research question of this study is:

- What can geophysical geoarchaeology reveal about the archaeology and depositional history of the site of Klein Hoek 1, South Africa?

The secondary research questions are:

1. What stratigraphic units are the bifacial points associated with?
2. To what extent is electrical resistivity tomography able to identify the stratigraphy at Klein Hoek 1?
3. Is electrical resistivity tomography able to detect any archaeological evidence within the deep layer of semi-consolidated sand at Klein Hoek 1?
4. How do variations in magnetic intensity at Klein Hoek 1, as revealed by the gradiometer, represent the archaeology and stratigraphy of the site?
5. How does the stratigraphy of the eroded portions of Klein Hoek 1 compare to the stratigraphy where erosion is limited?
6. How useful are geophysical techniques, such as electrical resistivity tomography and magnetometry, in understanding stratigraphy in an open site?

1.2 Thesis Outline

Chapter 2 contains an overview of Klein Hoek 1 and the Doring River Catchment in South Africa. Archaeology, geography, geology, and climate of the site and region are discussed.

Chapter 3 of this thesis provides a history and summary of southern African archaeology, specifically within the Doring River Catchment and discusses several key studies. This chapter also examines issues of the focus of rock shelter sites over open-air sites and the scarce utilisation of geophysical methods.

Chapter 4 provides an overview of the methods utilised in this research project. This includes tomographic survey and the geophysical techniques; electrical resistivity tomography, magnetometry and magnetic susceptibility. The theory, instrumentation, data collection and data processing methodology for each geophysical technique is discussed here.

Chapter 5 outlines the results of each geophysical technique utilised in the survey of Klein Hoek 1 and the anomalies detected in each dataset. This includes the Wenner and Dipole-dipole arrays for all three electrical resistivity topography surveys, the twenty grids created by the magnetometry survey, and the results of the four magnetic susceptibility tests.

Chapter 6 discuss the results of the electrical resistivity tomography survey, magnetometry survey, and magnetic susceptibility tests from the previous chapter. In this chapter, the results of each method are interpreted using knowledge of Klein Hoek 1's geology, topography, and archaeology, and compared to the results of the other geophysical techniques.

Chapter 7 will summarise the main points of this research project, discuss the limitations of the geophysical survey, and consider the direction of further research at Klein Hoek 1.

2 Study Area

Klien Hoek 1

This study focuses on the KH1 (KH1) open-air site, which is located on the Doring River in South Africa (Figure 1). The northern end of this MSA site is defined by a large point bar and the bank of the Doring River, while the southern boundary of the site is defined by a scree slope at the base of a siltstone cliff (Ames et al. 2020b:4; Figure 2). To the east of KH1 is a fence line, which is often used to mark the eastern end of the site (Figure 2). On the other side of the fence line, there is limited erosion and no visible archaeology on the surface, but there is likely archaeology in the subsurface (Shaw et al. 2019:413). The site is approximately 19,432m² and sits between 9m and 17m above the Doring River (Shaw et al. 2019:413).

Figure removed due to copyright restriction

Figure 1: Location of Klein Hoek 1. a) Archaeological survey area. b) Doring River Catchment and location of Klein Hoek 1 within it. c) Regional context of the Doring River catchment (Ames et al. 2020b:3).

The surface of KH1 is made up of both loose and indurated aeolian sediments with sparse vegetation and a few mounds, under which is a cobble bed that likely formed before the downcutting of the current river channel (Ames et al. 2020b:2). Under the

loose, unconsolidated aeolian sediment is a layer of semi-consolidated aeolian sand, which is roughly 6 metres thick. Under this stratigraphic unit is the bedrock, which is topographically complicated, likely due to erosion from paleochannels of the Doring River.

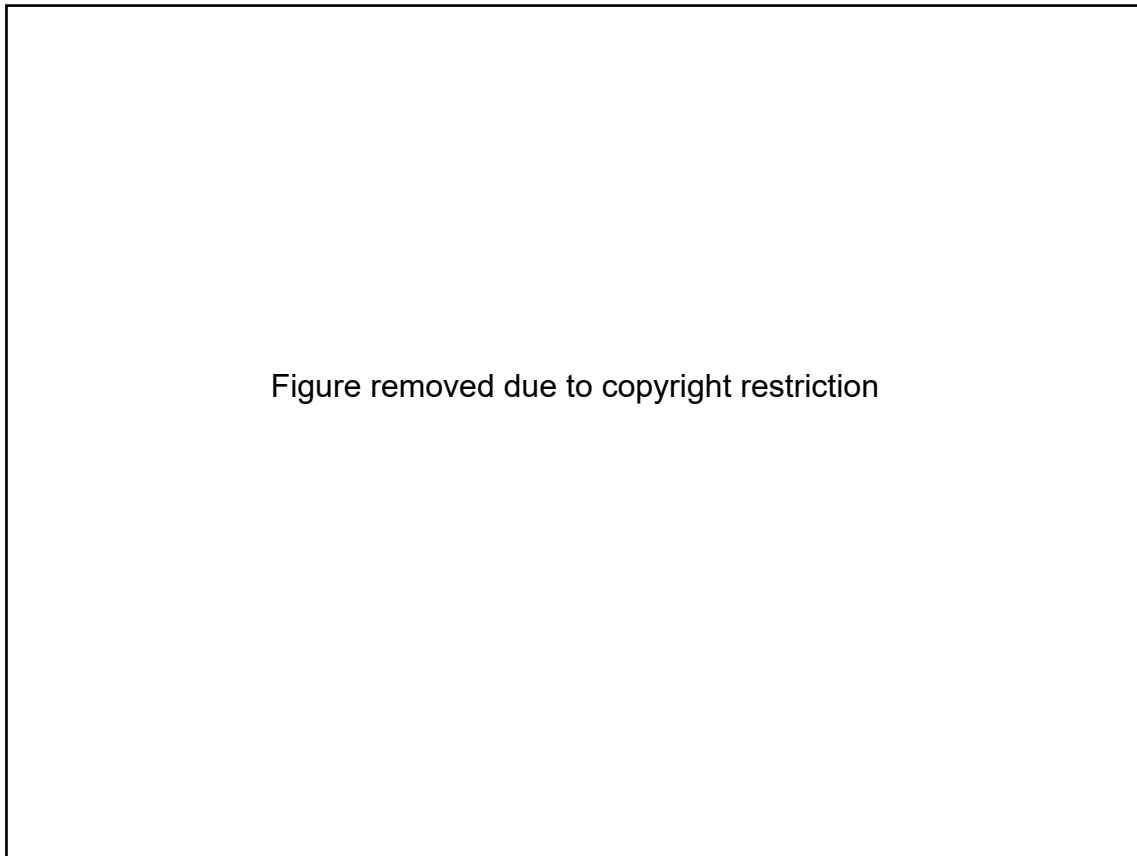


Figure 2: Oblique view of Klein Hoek 1 looking south, with a white line representing the border of the site and the location of the fence line, scree slope, basal cobble bed (point bar), and heuweltjies indicated (Ames et al. 2020b:4).

The archaeology primarily consists of stone tools created from blue-grey quartzite which are abundant on the eroded surface of the site (Ames et al. 2020b:2). A total of 6,747 artefacts have been mapped at KH1, the majority of which are attributed to the Still Bay, Post-Howiesons Poort, and Later MSA technocomplexes (Ames et al. 2020b:3; Shaw et al. 2019:414). The MSA artefacts are more common on the western portion of the site, while some Pleistocene LSA artefacts have been found

on the eastern side (Shaw et al. 2019:414). A small number of Howiesons Poort and Early MSA have been discovered at the site (Shaw et al. 2019:414).

Figure removed due to copyright restriction

Figure 3: The artefacts and sediment bodies located across KH1. A) A selection of bifacial points from the Still Bay cluster. B) Engraved ochre (Shaw et al. 2019:415).

There is a dense surface cluster of over 256 artefacts, including stone tools and worked ochres pieces, located between two mounds in the north of the site (Figure 4; Shaw et al. 2019:414). This cluster is quite significant as it appears to be eroding out from a buried context, potentially an old soil horizon, but still maintains coherency (Figure 3). As the bifacial cluster is seemingly fresh, an excavation has the potential to find in-situ layers underneath it, which would be important for the study of open-air sites in the region. The cluster includes many bifacial points from different stages of manufacturing, with around 100 of the artefacts found believed to be in the early stages of production (Shaw et al. 2019:414). Furthermore, many of the flakes found

across the site are associated with the construction of points (Shaw et al. 2019:414). These two features, and the proximity of KH1 to the Doring River, make it seem likely that the site was a location where early humans would create stone tools before travelling further into the catchment. The study of this bifacial cluster could be quite significant as it could reveal information on raw material procurement and Still Bay production. Thus, a geophysical survey of KH1 and the bifacial cluster could provide a unique snapshot of the past, that a rock shelter could not, and assist other open-air studies in the region.

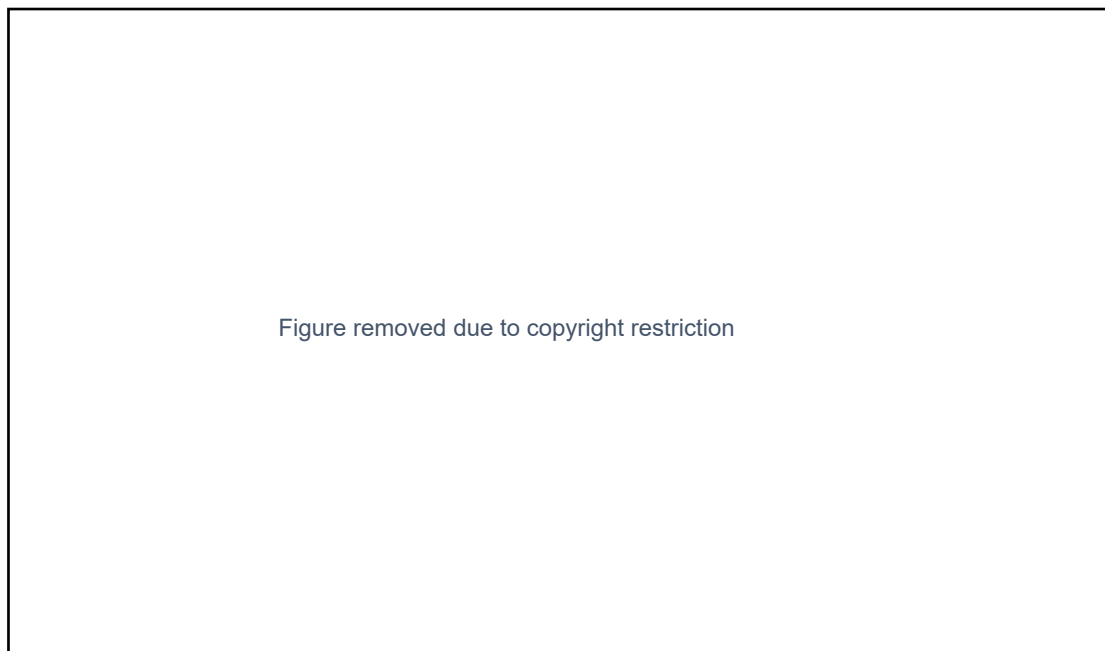


Figure 4: Photo of Klein Hoek 1, looking northeast, with the location of the stone tool cluster (Mackay et al. 2018:27).

The Doring River Catchment

The Doring River is located in the Western Cape of South Africa, currently located in the Winter Rainfall Zone (Ames et al. 2020b:2). It is a strongly seasonal river that typically starts to flow around May and June and ceases around November and

December when it is diminished to a series of shrinking waterholes (Shaw et al. 2019:402). The Doring River Catchment drains roughly 28,000km² of semi-arid shrubland, which normally has <250mm of rainfall per year (Ames et al. 2020b:2; Shaw et al. 2019:402). The river is in a rain shadow on the eastern side of the Cederberg Mountains, which are drained by its western tributaries. The Doring River's eastern tributaries are wide, braided streams that only flow with heavy rainfall. At the location of KH1, the Doring River is confined between cliffs formed in Devonian aged sediments from the Bokkeveld Group. The geology of the broader catchment is comprised of alternating shale and sandstone/quartzite layers from the Nardouw, Bokkeveld, and Witteberg formations (Ames et al. 2020b:2; Shaw et al. 2019:402). The soil within the catchment is typically sandy, acidic, and low in nutrients which when combined with the low annual rainfall has made the area poor for agriculture (Shaw et al. 2019:402). This is evident in the various abandoned European stone structures that dot the region (Shaw et al. 2019:402). Land use of the site extends back to the Middle Pleistocene and archaeological material is generally found in isolated sediment stacks that have been produced by aeolian and fluvial processes (Ames et al. 2020b:2; Shaw et al. 2019:402). The bedload of the river includes abundant cobbles of quartzite and hornfels, rare cobbles of silcrete and small pebbles and chert and quartz (Shaw et al. 2019:402). In the past, the Doring River would not only have been an important source of water for the region, but also a source of raw materials for the creation of stone tools.

3 Literature Review

Southern African archaeology has enjoyed a long history of research thanks to the abundance of well stratified, rich sites that occupy the area and a record that extends over at least 3 million years (Shaw et al. 2019:401). The Middle Stone Age (MSA) of southern Africa is particularly significant due to it being one of the earliest locations of behaviourally modern humans (Wurz 2013:305). However, the archaeological research of this period is dominated by the study of rock shelters and cave sites, at the expense of open-air sites (Ames et al. 2020b:1; Shaw et al. 2019:401). This has created a perspective of the MSA which is skewed in favour of rock shelter sites and thus limited and biased.

Figure removed due to copyright restriction

Figure 5: Map of significant late Pleistocene sites in southern Africa.

3.1 The Technocomplexes

The Stone Age is a broad period of prehistory which is characterised by the use of stone tools, which ended with the introduction of metalworking. In southern Africa, the Stone Age is divided into three parts, the Earlier Stone Age (ESA) which began around 2 Ma, the Middle Stone Age (MSA) which began between 500 ka and 250 ka, and the Later Stone Age (LSA) which began between 44 ka and 26 ka but differs across southern Africa (Shaw et al. 2019:401). The ESA in South Africa is dominated by heavy-duty cores and flake tools, generally made from coarse-grained rock, such as quartzite (Hallinan and Parkington 2017:331). The Fauresmith technocomplex is transitional between the ESA and MSA and is associated with the co-occurrence of hand axes, blades, and points (Lombard et al. 2012:139; Wurz 2013:306). As the MSA begins, hand axes disappear from the record and there is a notable increase in the production of cores using the Levallois technique (Hallinan and Parkington 2017:332). Other lithic technology changes include radial cores, producing flakes with convergent scars, faceted platforms, and blade production (Hallinan and Parkington 2017:332). Finally, the primary characteristic of the lithic technologies of the LSA is a shift to bipolar knapping techniques, microlithic technologies, and an increase in the range of raw materials utilised (Backwell et al. 2018:420).

The MSA is further divided into technocomplexes, defined by lithic technologies; Early MSA, Klasies River, Mossel Bay, Still Bay, Howiesons Poort, Post-Howiesons Poort, and Late MSA (Shaw et al. 2019:401; Table 1). A variety of lithologies can be found within Early MSA assemblages, with the most common being quartzite, and contain knapping systems with evidence of flakes, blades, and convergent flakes (Mackay et al. 2014:44). A notable characterisation is the inclusion of discoidal and Levallois flake technologies in this technocomplex (Lombard et al. 2012:139).

Notable Early MSA assemblages have been discovered at sites including Blombos Cave, Border Cave, Florisbad, Kathu Pan, Pinnacle Point, and Wonderwerk Cave (Lombard et al. 2012:139). Klasies River, also known as MSA I, spans from roughly 130ka to 105ka and is characterised by recurrent blade and reduction and convergent flake production (Lombard et al. 2012:138–139; Wurz 2013:308). From around 100ka to 80ka the Mossel Bay, also known as MSA II, technocomplex occurred (Lombard et al. 2012:138; Wurz 2013:308). Mossel Bay is characterised by a unipolar recurrent Levallois point and blade reduction process and prominent percussion bulbs (Lombard et al. 2012:138; Wurz 2013:308).

Still Bay is estimated to have started around 75 ka and ended around 70ka (Ames et al. 2020b:3; Jacobs et al. 2013:593; Mackay et al. 2014:44). Still Bay represents a shift to the manufacture of bifacial points, the advent of pressure flaking, and an increase in the use of fine-grained rocks, most notably silcrete (Mackay et al. 2014:44; Mackay et al. 2018:15). Notable Still Bay sites include Blombos Cave, Sibudu, Peers Cave, Diepkloof Rock Shelter, and Hollow Rock Shelter (Lombard et al. 2012:138; Mackay et al. 2014:44; Mackay et al. 2018:15). There are indicators that Still Bay ended around 70 ka, and while the following developments are unclear, it is believed that an occupational hiatus occurred for roughly 5 thousand years until Howiesons Poort began around 65 ka (Mackay et al. 2014:44; Mackay et al. 2018:15). The main indicator of Howiesons Poort is backed artefacts and small blades produced from unipolar prepared cores but also includes notched flakes and evidence of heat-treated silcrete (Mackay et al. 2014:44; Mackay et al. 2018:15). Notable assemblages have been discovered at Diepkloof Rock Shelter, Klein Kliphuis, Klasies River, Sibudu, Klipfonteinrand, and type site, Howieson's Poort Shelter (Lombard et al. 2012:194–195; Mackay et al. 2014:44). The technocomplex

ended around 58 ka when Post-Howiesons Poort began (Ames et al. 2020b:3; Mackay et al. 2014:45). Post-Howiesons Poort represents a gradual shift from backed artefacts to unifacial points and scrapers (Mackay et al. 2014:45; Mackay et al. 2018:17). Finally, the Late MSA technocomplex is estimated to have lasted from 50 ka to 25 ka and is characterised by its large variety of points, including hollow-based points, bifacial points, and unifacial points. (Ames et al. 2020b:3; Mackay et al. 2014:45; Shaw et al. 2019:404).

One of the earliest technocomplexes of the Later Stone Age (LSA) is the Robberg industry. This technocomplex lasted from roughly 23-22 ka through to around 11-10 ka (Porraz et al. 2016:204). The main characteristic marker of the Robberg industry is microlithic technologies centred around unmodified bladelets from single platform cores (Porraz et al. 2016:204). There is a prominence of standardisation and bipolar percussion during this technocomplex (Porraz et al. 2016:204).

Table 1: Technocomplexes of the Middle Stone Age.

Technocomplex	Date Range Estimates	Characteristics
Early MSA	300ka to 130ka	Prepared-core techniques, such as discoid, Levallois, and blade methods. Wide variety of rock types utilised, but most often quartzite.
Klasies River (MSA I)	130ka to 105ka	Recurrent blade and reduction and convergent flake production. Low frequencies of retouch.
Mossel Bay (MSA II)	100ka to 80ka	A unipolar recurrent Levallois point and blade reduction process. Prominent percussion bulbs.
Still Bay	75ka to 70ka	Bifacial points, fine-grained rocks, and evidence of pressure flaking.
Howiesons Poort	65ka to 58ka	Backed artefacts, small blades produced from unipolar prepared cores, notched flakes, and heat-treated silcrete.
Post-Howiesons Poort	58ka to 50ka	A gradual shift from backed artefacts to unifacial points and scrapers.
Late MSA	50ka to 25ka	A wide range of points, including hollow-based, bifacial, and unifacial points.

3.2 Rock Shelters vs Open-Air Sites

While southern Africa contains many significant MSA rock shelter sites, such as Blombos Cave and Diepkloof Rock Shelter, there is a distinct lack of open-air research in the region. This is a significant issue within MSA southern African archaeology, as research is heavily skewed in favour of rock shelters and cave sites, at the expense of open-air sites. (Fuchs et al. 2008: 425; Phillips et al. 2019:5852; Shaw et al. 2019:401). Southern Africa contains many significant MSA open-air sites such as, Anyskop, Duinefontein 2, Florisbad, Geelbek Dunes, Hackthorne Plateau, Hoedjiespunt, Kathu Pan, Putslaagte 1, Sea Harvest, Soutfontein 1, Tweefontein, and Uitspankraal 7 (Hallinan and Parkington 2017: 327).

The disparity of research skews heavily in favour of rock shelters over open-air sites has occurred for a few reasons. The first is that rock shelters provide exceptional preservation of the archaeological record and neatly stratified sequences (Ames et al. 2020b:1; Fuchs et al. 2008:425–426; Shaw et al. 2019:401). The second reason is the concern that open-air sites have lost their integrity due to erosion and rapid accumulation (Ames et al. 2020b:1; Mackay et al. 2014:43). Due to the arid environment of southern Africa, many open-air sites often occur in deflated contexts, which makes them more difficult to date when compared to the potentially uneroded stratigraphy found in rock shelter sites (Mackay et al. 2014:43–44). However, these two issues are part of another problem, that research funds in archaeology are limited (Ames et al. 2020b:1). This means funds are allocated to sites that will provide a greater informative return of time and costs. Rock shelter sites with great preservation and easy to access stratigraphy have been prioritised over deflated and scattered open-air sites because they are perceived as being more cost-effective and time-effective to study (Ames et al. 2020b:1). Another factor that dissuades the

study of open-air sites is that they usually occur in an environment that humans did not occupy alone (Kandel and Conard 2013:45). Animals die naturally in open-air environments and thus animal remains found in an open-air site may not be indicative of human activity. (Kandel and Conard 2013:45). This is also true for indicators of burning found in open-air contexts, which may have just been caused by bushfires (Kandel and Conard 2013:45).

This disparity of research represents one of the largest research gaps in southern African archaeology. A major problem is that rock shelter sites represent discrete spatial points in the landscape and do not likely represent the full range of human activities and behaviours in the past (Fuchs et al. 2008:426; Phillips et al. 2019:5853; Shaw et al. 2019:401). Activities such as the acquisition of food and water, the manufacture of tools and other objects, and sometimes social practices likely mostly took place within an open landscape context (Mackay et al. 2014:44). This is a major limitation when the majority of excavations in southern Africa have occurred on rock shelters (Shaw et al. 2019:401). While this may provide rich data due to the natural preservation and stratigraphic properties of rock shelters, it fails to reveal patterns of land use and settlement organisation on a regional level (Shaw et al. 2019:401).

Another problem with this approach is that rock shelters may have been unoccupied by humans throughout prehistory (Mackay et al. 2014:44). In some periods, rock shelters seem to have been utilised more often, leading to an overrepresentation of them during these periods, i.e., the MSA (Mackay et al. 2014:44).

Recently the emphasis on rock shelters in southern African archaeology has been called out by some archaeologists that claim it has provided a limited scope to interpretations of the past (Ames et al. 2020b:1; Fuchs et al. 2008:426; Mackay et al. 2014:44; Phillips et al. 2019; Shaw et al. 2019:401). This has led to a surge of open-

air site studies within the region to provide a greater understanding of the past. An example of this is the Geelbek Dunes open-air site which has recently been the subject of many studies ranging from settlement dynamics, land use and economics (Dietl et al. 2005; Fuchs et al. 2008; Kandel and Conard 2005; Kandel and Conard 2013). Other recent open-air sites studies include, Uitspankraal (Low et al. 2017; Watson et al. 2020; Will et al. 2015), Putslaagte 1 (Mackay et al. 2014), Hoedjiespunt 1 (Kyriacou et al. 2015; Will et al. 2013), and Anyskop (Dietl et al. 2005). The Doring River Archaeology Project was established with the objective to study the evolution of human land use during the Late Pleistocene and Holocene by integrating rock shelter sequences and open-air data (Shaw et al. 2019:402). There have also been investigations on the erosional properties of the Doring River catchment to identify which sites and scatters are under imminent threat of erosion and which remain intact (Ames et al. 2020b:2). This research will assist in providing a better understanding of open-air sites and assist in making them more available to research (Ames et al. 2020b:2).

3.3 Archaeology in the Doring River Catchment

Doring River Archaeology Project

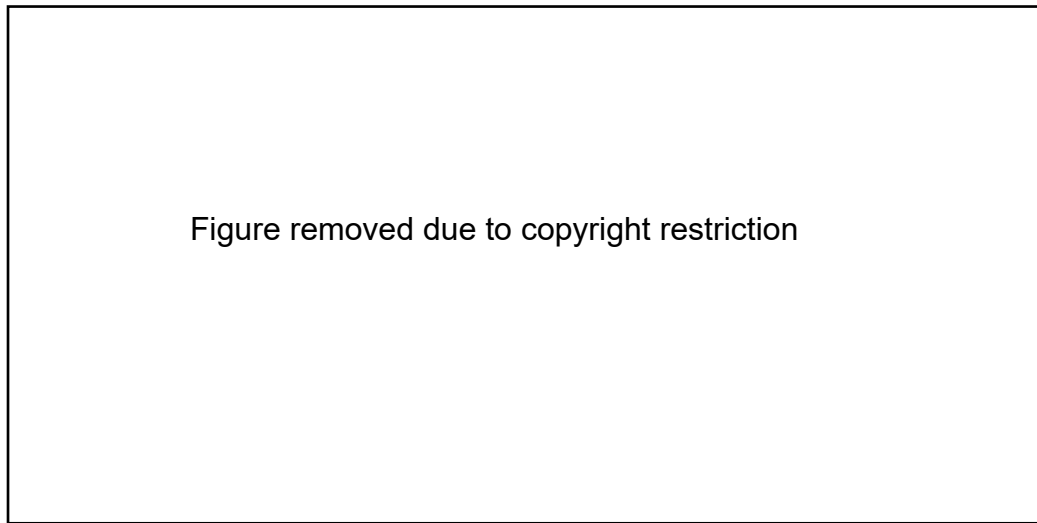


Figure 6: Map of South Africa showing the location of the Doring River Archaeology Project study area. Circles = rock shelters. Squares = open-air sites. EB = Elands Bay, DPK = Diepkloof, KK = Klein Kliphuis, KFR = Klipfonteinrand, MRS = Mertenhof (Ames et al. 2020a:395).

The Doring River Archaeology Project is responsible for most of the recent archaeological research in the Doring River catchment. The project aims to record and examine archaeological material along the Doring River to gain a better understanding of land use during the Late Pleistocene and Holocene (Shaw et al. 2019:405). The project was inspired by the threat of erosion destroying the stratigraphic context of sites in the area due to the modern climate conditions and land use practices. In 2018, the first stage of the project began with surface surveys at KH1, Doringbos 8, and Uitspankraal 9 (Ames et al. 2020a:3; Watson et al. 2020:). In 2019 the team continued their surveys but created an offline-capable, cloud-based mobile GIS system to speed up the process (Ames et al. 2020a:14). Over 2018 and 2019 the project documented at least 24,220 artefacts across six localities (Ames et al. 2020a:14; Shaw et al. 2019:407). As of 2019, the rock-shelter sites of Klipfonteinrand 1, Klipfonteinrand 2, Mertenhof, Hollow Rock Shelter, and Putslaagte

8 and the open-air site of Putslaagte 1 have been excavated (Low and Mackay 2018:172-174; Shaw et al. 2019:404; Watson et al. 2020:211-212).

The Doring River Archaeology Project has also conducted research into the erosional characteristics of the region (Ames et al. 2020b). This investigation aimed to identify the erosional impact on the scatters at open-air sites to understand which sites had lost their integrity, which retain integrity, and which are under threat of losing integrity due to erosion (Ames et al. 2020b:2). In regards to KH1, the study found that while the northern indurated mounds seem to have protected part of the site from erosional effects for a time, they are coming under increasing threat (Ames et al. 2020b:13). The study also concluded that the Still Bay artefacts at KH1 have retained considerable spatial integrity, giving them a high potential for future research (Ames et al. 2020b:13).

The project has also researched the surface disaggregation of miniaturised stone tools, which are associated with the Later Stone Age of southern Africa (Phillips et al. 2019:5855). This was completed by placing a collection of replica miniaturised flakes and cores within an archaeologically sterile environment in the Doring River catchment and observing their movement over 22 months (Phillips et al. 2019:5855-5856). The study found that both bipolar and freehand cores and flakes had comparable movement patterns, which is evidence against the theory that the occurrence of bipolar technology between rock shelters and open-air sites is due to differential preservation of the stone tools (Phillips et al. 2019:5874).

Gearing Up Theory

In 2018, an analysis of Robberg blades and blade cores from three rock shelters, Putslaagte 8, Klipfonteinrand and Mertenhof was conducted (Low and Mackay 2018). The study found a negative correlation between the distance from the Doring River and the abundance of hornfels and silcrete blades in a site (Low and Mackay 2018:188). At the same time, the more distant sites contained a high number of local quartz tools and higher blade to blade core ratios than sites closer to the river (Low and Mackay 2018:188–189). As the Doring River is a source of hornfels and silcrete the study concluded that the data showed that sites close to the river were ‘gearing up’ locations, where tools would be prepared and then transported deeper into the catchment (Low and Mackay 2018:189). However, the study had a problem in that it did not include a site directly on the Doring River for comparison to the other three sites (Watson et al. 2020:212).

As part of the Doring River Archaeology Project, a study was conducted at Uitspankraal 9, an open-air site located on the river with a rich Robberg assemblage (Watson et al. 2020:212). They found that there was a higher number of hornfels and silcrete tools and a lower number of quartz tools compared to the sites in the previous study (Watson et al. 2020:224). This reinforces Low and Mackay’s conclusion that the Doring River was used as a manufacturing point for tools that would then be transported further into the catchment (Low and Mackay 2018:189; Watson et al. 2020:223-4).

Another study at Putslaagte 1, an open-air site, found that there is a cortex deficiency at the site (Lin et al. 2016:177). This is an indicator that many stone tools created at the site were transported away from it (Lin et al. 2016:178). The study compared this to assemblage at the rock shelter, Putslaagte 8, and found that it had

an abundance of flakes (Lin et al. 2016:178). However, the cortex ratio of the stone tools at Putslaagte 8 was not high enough to account for the cortex deficiency at the open site. Thus, it is improbable that every stone tool exported from Putslaagte 1 was transferred to the rock shelter, implying that the transport of lithics was not just from one point to another point and that artefacts were transported over long distances, further away from the Doring River (Lin et al. 2016:178).

Putslaagte 1

While there have been excavations at a few rock shelters within the Doring River catchment, only a single open-air site has been excavated (Shaw et al. 2019:404). This site is Putslaagte 1, where in January 2011 a single test excavation was conducted with the goal of creating a controlled assemblage to characterise the site and understand its formation (Mackay et al. 2014:47). The test pit was created 2 metres by 1 metre and reached a depth of roughly 1.3 metres in one half and 1.8 metres in the other half (Mackay et al. 2014:47; Figure 7).

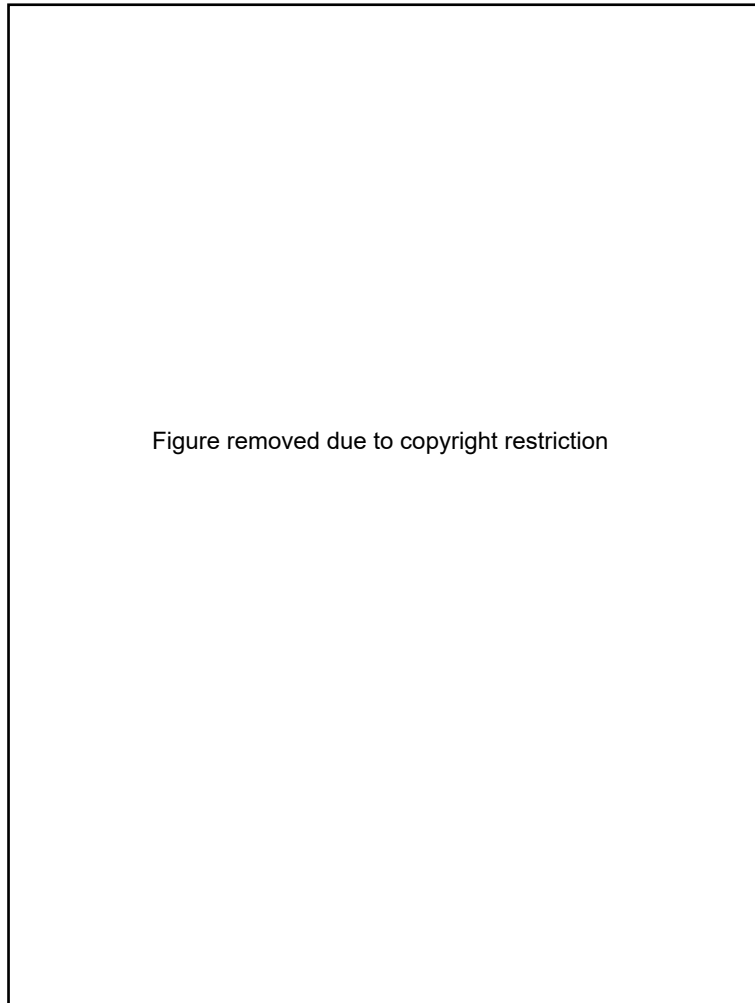


Figure 7: Western side of the test pit at PL1 with the location of OSL samples and proposed paleosol location (Mackay et al. 2014:48).

One of the findings of this study was that the area excavated had an artefact density of around 3350 artefacts/m² and using this, they estimated that the rest of the site had at least 350,000 artefacts remaining (Mackay et al. 2014:53). This artefact density is similar to other sites along the Doring River and indicates that the region was intensely occupied during the MSA (Mackay et al. 2014:53). However, excavations of rock shelters within the region have displayed a lack of evidence of human occupation during the same period, which caused many to believe that the region was abandoned during the MSA (Mackay et al. 2014:55). The results from this test excavation at Putslaagte 1 suggest that there was a population redistribution

to areas adjacent to a water source and away from rock shelter sites, rather than a complete abandonment of the region (Mackay et al. 2014:55). This is an example of how the focus on rock shelter research can create a biased and incorrect interpretation of the past.

The other significant finding was that the lithic technologies of the site were characteristically MSA but differed from those found at other sites in the catchment. The biggest difference was the lack of any characteristic markers of the Still Bay, Howiesons Poort, or post-Howiesons Poort technocomplexes which are commonplace at many other MSA sites (Mackay et al. 2014:46). This indicates that there may have been local variants of lithic technology within the later MSA and may explain why there have been difficulties characterising a late MSA technocomplex (Mackay et al. 2014:56).

Uitspankraal 7

During October 2014 and March 2015, a survey was performed at the open-air site, Uitspankraal 7 (Low et al. 2017:382). The site consists of a sediment stack located on top of a cobble terrace with a modern dune crest located on the eastern end of the site (Shaw et al. 2019:411). On the western and southern portions of Uitspankraal 7, there are deep rills that cut into the sediment and expose the oldest stratigraphic unit at the site; indurated red sediments with nodular calcrete (Shaw et al. 2019:411). Above this unit is a layer of partly consolidated yellow sand, which is in turn covered by the unconsolidated dune sands (Shaw et al. 2019:411). This survey marked the location of any stone artefacts that measured more than 20 mm and noted certain characteristics about it such as material type and weight (Low et

al. 2017:382). Over 3078 artefacts were examined over the two survey field seasons (Low et al. 2017:384). The results were combined with results from another survey at Putslaagte 8, and together they documented a new expression of the Early Later Stone Age technocomplex in the local Doring River region (Low et al. 2017:402). This is comparable to the study at Putslaagte 1 which suggested there may have been local variants of lithic technologies in the late MSA (Mackay et al. 2014:56). This is an important factor to keep in mind when researching KH1 as it could very well have a different local expression to other sites in the region.

3.4 Geophysics in South Africa

Geophysical surveys within archaeology are quite common in some parts of the world, such as North America and Europe (Magnavita 2016:116). However, the application of these surveys in southern Africa has been quite limited (Magnavita 2016:118). Even within Africa, there is a disparity between the number of geophysical surveys conducted in Northern Africa and Sub-Saharan Africa. Between 1994 and 2015, there were 17 articles published on North Africa, 15 of these on Egypt, in the archaeological geophysics journal, *Archaeological Prospection* (Magnavita 2016:119). Meanwhile, in the same time frame, there were only 2 articles on Sub-Saharan Africa (Magnavita 2016:119). One of the earliest geophysical surveys in southern Africa was at an Early Iron Age site, Ndongwane, in 1996 (Fowler et al. 2004:445; Magnavita 2016:124). Here they conducted an electromagnetic survey to better understand spatial patterns, size, depth and archaeology of the site (Fowler et al. 2004:445-446; Magnavita 2016:124). Another early site where geophysical techniques were employed is Fort Eshowe, where in 1999, electrical resistivity tomography and gradiometer surveys were performed

(Magnavita 2016:125; Pollard et al. 2013:150). The goal of these surveys was to examine the accuracy of fort plans drawn by the Royal Engineers in 1879 (Pollard et al. 2013:150).

More recently there have been some geophysical surveys on Stone Age sites within the region. Two examples of these are the sites of Bestwood 1, an open-air site located in the Northern Cape and Drimolen, a cave site located in the Cradle of Humankind. Ground-penetrating radar and magnetometry surveys were conducted at Bestwood 1 (Papadimitrios et al. 2019:1). The study found that the geophysical survey was able to successfully provide data on the stratigraphy and the magnetics, in particular, was able to identify a paleochannel beneath the site (Papadimitrios et al. 2019:6). As past occupation would have likely occurred in close proximity to water, knowing the location of the paleochannel will assist future excavations in locating archaeological material by focusing on the banks of the channel (Papadimitrios et al. 2019:6-7). At Drimolen, a hominin fossil site, ground-penetrating radar surveys were combined with ground-truthing and photogrammetry to characterise stratigraphy and deposits (Armstrong et al. 2021:1). The survey was successful with the data revealing various features in the subsurface including a chert layer, which is likely part of a collapsed roof, and an area of infilled material for future study to focus on (Armstrong et al. 2021:8,10). Both of these examples show that geophysical surveys can be successful in the arid context of South Africa. Bestwood 1 specifically shows that applying geophysics to an open-air arid site can provide valuable data that can assist in future excavations of the site.

Within the Western Cape of South Africa, there have only been a small number of geophysical surveys. One of the only examples of geophysics in the region is a project at a rock shelter site called Elands Bay Cave (Miller et al. 2016). This project

utilised ground-penetrating radar to map out the depth of bedrock across the site and study the site formation (Miller et al. 2016:76-77). The results from the survey provided significant data on the morphology of the site such as revealing that the bedrock in the walls and ceiling continued into the floor of the rock shelter creating a basin-like formation in the base of the shelter, which had been filled by sediment (Miller et al. 2016:121). However, there have been no published geophysical surveys on sites along the Doring River or within its catchment. This is significant as many sites within the catchment have been or are being studied and a better understanding of the stratigraphy of the region could assist these investigations.

3.5 Summary

Southern Africa archaeology is significant as it contains some of the earliest known and richest hominin sites, including some of the earliest evidence of drawing and symbolism. However, there is a large gap in this archaeology which is the focus of research efforts on rock shelter sites rather than open-air sites. Many rock shelters likely do not represent all past human activities and behaviours, which has created an interpretation of the southern African prehistoric past that is biased and possibly incorrect. This is due to it being more difficult to know where to excavate on open-air sites which can lead to them being more costly, time-consuming and difficult to study than rock shelters. This is significant when there is only a limited amount of research funding available. Recently the disparity between rock shelter and open-air site research has been called out by archaeologists, and while there has been a push to integrate open-air data with rock shelter sequences, there is still currently a lack of published open-air research. Within the Doring River catchment, there has only been one excavation at an open-air site, meanwhile, six rock shelters have been

excavated. A geophysical survey at KH1 will contribute to southern African archaeology by providing a unique snapshot of the past and helping in understanding open-air sites within the Doring River region. The survey will also be a test of geophysical techniques within the southern African context, which has seen a limited implementation of geophysics. If geophysical techniques are successful at KH1, they could be utilised more widely in southern Africa, contributing to open-air research by providing a greater understanding of them and making them more cost-effective to excavate.

4 Methods

4.1 Topographic Survey

For this project, all topographic surveying was performed using an Emlid Reach RS+ RTK-GPS, which consisted of a base station and rover unit. Real-Time Kinematic – Global Positioning System, or just simply RTK, is a satellite-based navigation system (Idris 2019:324). The device requires line-of-sight to at least five satellites in order to provide accurate measurements (Idris 2019:324). However, when this is achieved, the RTK can provide more accurate and quicker measurements than other alternative methods, such as a total station (Idris 2019:324). An open-air site, such as KH1, where there are very few obstacles to obscure satellite coverage is the optimal environment for RTK. The base position of the RTK was determined in post-processing using the CSRS-PPP service, while the rover position was corrected using RTK-LIB software. Each ERT probe, magnetometry grid, and magnetic susceptibility test location was recorded with the ERT, which allows us to compare overlapping data. The RTK points were also combined with a drone survey done by Alex MacKay's team in an earlier field season, which allowed us to create a birds-eye-view of the site with the location of each geophysical survey.

4.2 Geological Mapping

A drone survey was conducted in 2018 using a DJI Mavic Pro with a predetermined flight path at 40 metres above the surface (Ames et al. 2020b:3). 11 ground control points, four of which are permanent, were placed across the survey area and recorded using an RTK before the drone survey. The 99 geotagged images created were imported into Agisoft Photoscan Version 1.4.5 (now Agisoft Metashape),

aligned together and a sparse point cloud was generated (Ames et al. 2020b:4). The coordinates for each ground control point were corrected to the correlating RTK collected points. Finally, a dense point cloud was generated at high quality, with an upper point limit of 60,000 and a lower point limit of 6000, from which an orthomosaic was produced (Ames et al. 2020b:4)

For this project, the orthomosaic was imported into ArcGIS for geological mapping. Each unit on the surface of KH1 was identified based on the drone photo as well as videos and photos taken during fieldwork. These geological units were then mapped out in ArcGIS by creating polygon features for each unit over the top of the drone photo. The geological map created from this process was utilised to assist in interpretations of the results from the geophysical survey.

4.3 Overview of Geophysical Techniques

Geophysical techniques measure the physical properties of the Earth (Bolger 2010:1). Traditionally, this discipline has been utilised for the large-scale exploration of economic resources such as groundwater, metals, and hydrocarbons within the Earth (Bolger 2010:2; Witten 2006:1). However, it has also found use in a wide range of other occupations such as in hydrology, palaeontology, environmental monitoring, geological mapping, construction, military, counterintelligence and intelligence, forensics, and counter-narcotics (Bolger 2010:2; Witten 2006:2). Within the last few decades, there has been a recognition among archaeologists for the need for non-invasive practices (Piro 2009:27). As non-renewable material culture became increasingly threatened by natural and human processes, archaeologists became aware that non-destructive and non-invasive techniques were of the utmost

importance (Piro 2009:27). This led to the adoption of geophysical ground-based survey techniques by archaeologists to map the subsurface of sites and located archaeological features (Campana 2009:15; Linford 2006:2210; Piro 2009:28). These methods are non-destructive and non-invasive, which makes them invaluable to archaeologists (Grassi et al. 2021:1).

Geophysical techniques measure specific physical properties within the Earth. These techniques can be divided into two categories, passive and active. Passive methods can be described as a method where the energy measured has been created by natural means or artificially for non-geophysical reasons (Witten 2006:1). The types of energy measured by passive techniques include magnetic fields, gravitational fields, and electrical fields produced by features in the subsurface (Piro 2009:28). Active methods are those where the energy measured is created for the singular purpose of the geophysical survey (Witten 2006:1). These methods inject signals, generally seismic, electrical, or electromagnetic, into the Earth and then measure the return signals and how they have been altered by features in the subsurface (Piro 2009:28). Two of the most commonly used active methods used in archaeology are electrical resistivity tomography (ERT) and ground-penetrating radar (GPR).

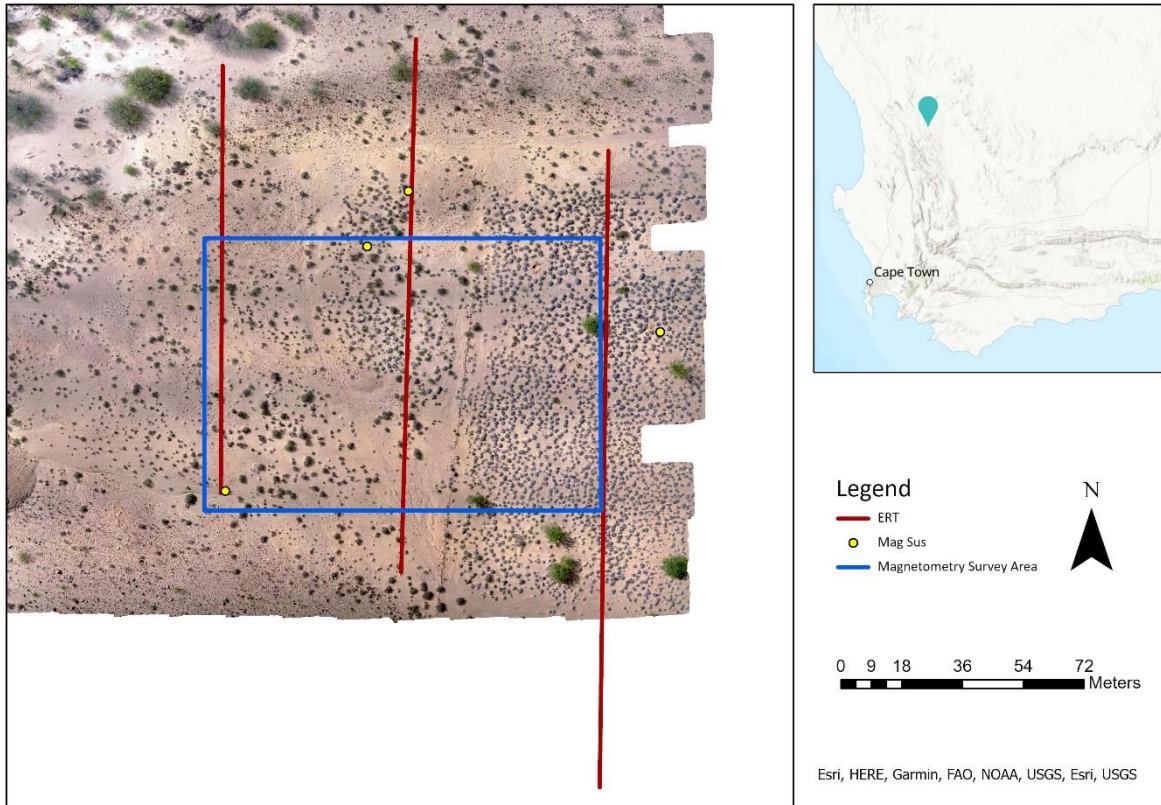


Figure 8: Site plan of KH1 showing the location of the geophysical survey.

4.4 Electrical Resistivity Tomography

Theory

Electrical resistivity tomography (ERT) is the injection and subsequent measurement of electrical current into the subsurface of the Earth. Archaeological features can alter the electrical current which can allow ERT to reveal and locate archaeology within the subsurface (Schmidt 2013:11). The most basic principle behind ERT is Ohm's Law ($V=IR$) which consists of three parts, current, voltage, and resistance (Witten 2006:300). Current is the measurement for the flow of electrons through an object or area and its unit is ampere or amp. Voltage is described as the work needed for an electrical source to move electrical current between two points and its unit is volts. Finally, the resistance of an object or material is how that object or

material impedes the flow of electrical current and it is measured in ohms. Critical to ERT is resistivity which is the property of a material with specific dimensions (Clark 1996:27). This means resistivity can be used to describe materials and compare them against each other in a standardised way which is the core of ERT surveying and allows for the identification of archaeology in the subsurface (Clark 1996:27; Schmidt 2013:17).

By injecting electrical current into the Earth and measuring the electrical resistivity, this technique can create a two-dimensional (2D) or three-dimensional (3D) model of the subsurface (Samouëlian et al. 2005:175; Touthmalani 2010:6441-6442).

Electrical resistivity measurements from different geological units in the subsurface provide a better understanding of the stratigraphy of a site or area (Barde-Cabusson et al. 2013:2544; Chambers et al. 2013:26; Cozzolino et al. 2018:10; Samouëlian et al. 2005:175). For example, materials with low resistance such as metal or clay can be distinguished from high resistance materials such as wood or dry sand (Table 2). The characterisation of the subsurface of an archaeological site provides valuable information about the site formation and can assist in identifying and locating archaeological material. A good example of this is an ERT survey at the Neolithic site of Szeghalom-Kovácsalom, in Hungary, where they used the results from the survey to create 2D and 3D models of the subsurface and map out the stratigraphy of the site (Papadopoulos et al. 2014:182). Other applications of ERT within archaeology include the investigation of subsurface caves (Witten 2006:316), the mapping of shipwrecks (Simyrdanis et al. 2018:2), and the detection of unmarked graves (Moffat et al. 2016:8).

Table 2: Indicative resistivities of common rocks and soil materials (Saad et al. 2012:371).

Figure removed due to copyright restriction.

Instrumentation

The ERT data for KH1 was collected using a ZZ Flash-Res Universal. The unit has 64 channels allowing for up to 64 electrodes to be used at a spacing of one metre.

Two arrays were chosen for this ERT survey, they were the Wenner array and the Dipole-Dipole array. The Wenner array is a four-electrode array that has two inner electrodes acting as potential electrodes and two outer electrodes serving as current electrodes (Hossain et al. 2018:19). This array is effective at identifying the vertical changes in resistivity within the subsurface, especially below the centre of the array, and has the highest signal strength of the two arrays utilised but is less sensitive to changes horizontally (Hossain et al. 2018:18; Milsom and Eriksen 2011:131). Dipole-dipole consists of two sets of electrodes, a set of potential electrodes and a set of current electrodes and maintains the same distance of each electrode in both sets (Hossain et al. 2018:19). Overall, this array is more sensitive to the horizontal changes in resistivity but is poor at identifying resistivity change vertically within the subsurface and has the weakest signal strength of these arrays (Hossain et al. 2018:18; Milsom and Eriksen 2011:131). Both of these arrays have their strengths and weaknesses that make them better at identifying different points in the

subsurface. For this ERT survey, these two arrays were chosen as the strengths of one array covers the weakness of another and overall, they provide an excellent picture of the resistivity in the subsurface.

Data Collection

While GPR can provide a high resolution of the stratigraphy of a site, ERT was chosen for this study, due to the belief that KH1 had a deep stratigraphy containing clay, which would significantly decrease the penetration depth of GPR. Data was collected using the Wenner and Dipole-Dipole Arrays using 120V for 1.2 seconds for each measurement and with an electrode spacing of one metre. This setup provided a penetration depth of roughly 20 metres. To decrease contact resistance, saltwater was poured over each electrode during set-up. Before acquisition, contact resistivity was measured to ensure high-quality data. If low conductivity was present, it would be increased with further saltwater or installing the electrodes deeper into the ground. Before an ERT line was completed, descriptive notes on each visible layer along the line were taken.

Three ERT survey lines were performed at the site, all of which ran north to south across the site and had an electrode spacing of one metre. The position of each survey line, including each individual electrode, was mapped using the RTK (Figure 9). The ERT lines were deliberately positioned to intersect three key features at the site; the point bar, the scree slope, and at least one of the mounds. This will allow the stratigraphy of these features to be compared to the stratigraphy of the rest of the site. One of the survey lines was also placed on the eastern side of the fence line, to see how the stratigraphy in that area compares to the eroded surface of KH1.

A fourth survey line was planned, which would run east to west and intersect the first three lines, however, due to technical problems this did not occur.

Line 1 was the most western line performed, running north to south, and consisted of three rolls bringing the line to a total length of 128 metres. This line started on the fluvial sediment of the Doring River, crossed over the bar feature and western most mound, before ending just before the scree slope. Line 2 was conducted around the centre of KH1, running north to south, and came to a total length of 160 metres. This line started in the river valley, just before the boulder bar, ran up the slope of the boulder bar, crossed one of the central mounds, passed the bifacial cluster, and ended just a couple metres short of the scree slope. Finally, line 3 was the most eastern line completed, taking place within the eastern side of the fence line where minimal erosion has taken place. Like the first two lines, it ran north to south and was comprised of five individual rolls which bring the line to a total of 192 metres in length. Line 3 starts at the bottom of a mound feature, crosses over the mound and into the modern unconsolidated sediment unit. The line continues through this layer for the majority of its length and finally, the last roughly 35 metres are located on the scree slope.

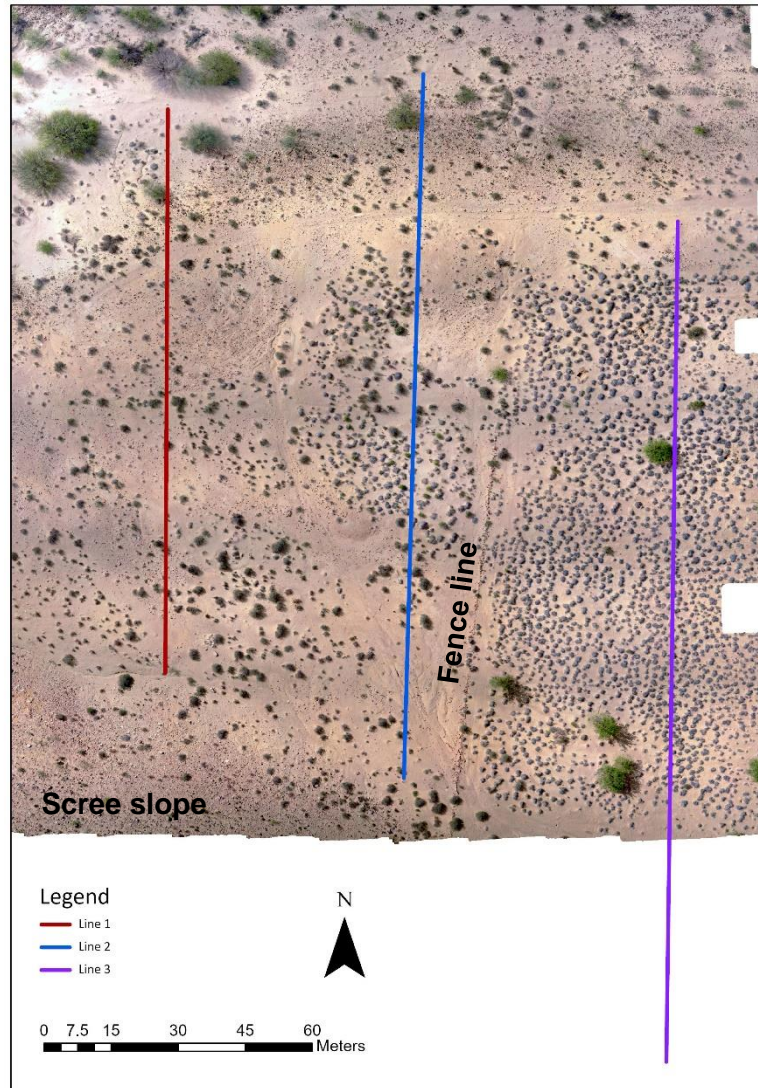


Figure 9: The location of the ERT survey at KH1.

Data Processing

During fieldwork, preliminary data processing was conducted to further our understanding of the site and assist in deciding where to conduct the next ERT survey.

During the data processing stage, the ERT data was first exported into individual arrays using the software ZZ-RdatacheckU64. Next, each array was filtered for high and low voltage to remove outliers and then converted into a Res2DINV format using

a custom spreadsheet. The elevation of each electrode, which was collected during the topographic survey, were added to the bottom of each array file. This allows for the final model to be spatially correct. Each array was opened in Res2DINV, a 2D inversion software created by Geotomo (Geotomo 2019). Repeated points were removed, and outlier points that had values much higher or lower than the neighbouring data points were exterminated using the Exterminate Bad Data Points function. This decreases the probability of any bad data points within the results, which could have been created by electrode failures or poor electrode ground contact.

The data was then inverted using the Robust Inversion Method in the Res2DINV software. Robust Data Constraint was chosen as this option reduces the influence that outliers have on the inversion result. For the model inversion constraint, the robust model constraint was selected as the subsurface of KH1 has strong boundaries due to the presence of bedrock and cobble sized fluvial sediment in the form of a point bar. This inversion constraint attempts to minimise the absolute changes in resistivity values, which makes it more suited to the subsurface of KH1. The extended model feature was turned off for the model discretization, the process of dividing the subsurface into cells for the inversion model. The data was finally inverted and the contour values for the 2D model was calculated using the Jenks Break function in R. The colour values were adjusted to better represent the contour values and make the model easier to read. This process was completed twice for each ERT line, one for the Wenner array and one for the dipole-dipole array, resulting in six ERT pseudo section models in total.

The goal of inversion is to create a model that gives a response that is similar to the measured data and geologically reasonable. This is due to electrical resistivity

tomography being a surface measurement from which the subsurface results must be derived. Res2DINV calculates the change in the model parameters, which will reduce the difference between the calculated and measured apparent resistivity values (Geotomo 2019:4; Papadopoulos et al. 2006:167). The result of this process is an idealized mathematical pseudo-section of the apparent resistivity within the earth.

4.5 Magnetometry

Theory

A magnetometer measures the magnetic field which is the “composite of mutual forces acting among the poles of two or more magnets (Witten 2006:75).” However, this process is too insensitive to detect weak anomalies in the near-surface which are common targets in archaeological investigations (Clark 1996:66–67; Witten 2006:88). Therefore, a gradiometer is utilised instead which consists of two magnetometers set a small distance apart, typically one above the other (Clark 1996:67; Witten 2006:89). A gradiometer is much more suited to surveying shallow features as it measures the gradient of a magnetic field by evaluating the difference between the values measured by the two magnetometers (Witten 2006:88).

Magnetic sources further from the gradiometer, such as a metal object deep in the subsurface, will affect both magnetometers almost equally, resulting in a much less prominent reading (Clark 1996:67; Witten 2006:88) However, shallow features will have a larger variation between the two magnetometers, resulting in a much stronger reading. Gradiometers are also less susceptible to diurnal and geological noise as interference will affect both sensors equally, thus resulting in the interference having no effect on the results (Clark 1996:67). The data collected by the gradiometer is

processed into a map of magnetic intensity that indicates potential prehistoric hearths, metal objects, or any other phenomena that may be archaeological (Cozzolino et al. 2018:36; Herwanger et al. 2000:849; Tousemalani 2010:6442-6443).

Human occupation and activities can cause the conversion of weakly magnetic iron-oxides and hydroxides into more magnetic forms within the soil (Dalan and Banerjee 1998:3). This effect was first described by Le Borgne in 1955 and can be caused by two processes (Schmidt 2007:3; Tite and Mullins 1971:209). The first process is when organic material is burned on the surface of the soil, temperatures can exceed the Curie point of iron-oxides and an oxygen-free environment can be created (Schmidt 2007:3). This creates a reducing atmosphere which causes the haematite in the soil to be converted into magnetite and then as it re-oxidises, it forms into maghemite (Dalan and Banerjee 1998:7; Maki et al. 2006:208; Schmidt 2007:3; Weston 2002:208). Since this process was first described, it has been proven that the level of magnetic enhancement depends on the temperature achieved by the fire, the porosity of the soil, the amount of organic material and iron in the soil, how often heating has taken place at the location (Dalan and Banerjee 1998:3).

The second process, which was described as the 'fermentation effect' by Le Borgne, can be described as the reduction of haematite to magnetite by the decomposition of organic materials within anaerobic soils and then the re-oxidisation to maghemite during aerobic conditions (Schmidt 2007:3; Tite and Mullins 1971:209). While for a time this process was believed to have little impact on the overall magnetic enhancement of soil, it is now believed by some to be as equally important to magnetic intensity as fire (Dalan and Banerjee 1998:4). However, the importance of

the 'fermentation process' to overall magnetic intensity is still debated (Dalan and Banerjee 1998:5; Fassbinder 2017:503; Weston 2002:208).

The magnetic intensity of soil can also be increased through the introduction of wood ash from the burning of hearths into that soil (Linford and Canti 2001:224; Maki et al. 2006:208). This is due to the presence of fine-grained iron-oxides in the wood ash which is then introduced into the soil (Linford and Canti 2001:223; McClean and Kean 1993:389-390). Archaeomagnetic studies of wood ash have been conducted at a few sites in South Africa, for example at Sibudu Cave in KwaZulu-Natal (Herries 2009:247).

Through these processes, the burning of a hearth creates a magnetic anomaly within the soil (Jordanova et al. 2019:735; Maki et al. 2006:208). This anomaly acts as a magnetic signature of the hearth which can then be identified and located within the subsurface using magnetometry. This is important as the detection of prehistoric hearths within a site can often locate areas where human occupation and activities occurred. This makes magnetometry surveys useful in identifying parts of the subsurface within a site where excavations are likely to yield archaeological material.

Instrumentation

Gradiometer data was collected using a Bartington Grad-601, a fluxgate gradiometer consisting of a DL601 Data Logger, a BC601 Battery Cassette, and one or two Grad-01-1000L cylindrical gradiometer sensors (Bartington a:6). These are mounted on a frame that has a Grad601-2 Carrying Harness attached to alleviate the weight on the operator's arms (Bartington a:16). For this magnetometry survey, two Grad-01-1000L sensors were used as this reduces the amount of time needed and distance

walked by half, allowing for a larger area to be surveyed (Bartington a:9). Both cylindrical sensors contain two fluxgate magnetometers exactly one metre apart (Bartington a:8).

Data Collection

A quick method of surveying was necessary for the large open-air site, for which magnetometry was utilised. The magnetic survey of large portions of the site will allow for the identification of hearths within the subsurface, where archaeological material may be found. Before the magnetometry survey was conducted all metal on the surface was removed from the study area. The gradiometer was set up and run for over 15 minutes to allow it to adjust to the environment as per the manual (Bartington a:17). As the Grad-601 is very sensitive to magnetic anomalies, the surveyors made sure to remove any items on their person that contained metal. After this adjustment period, the gradiometer was then balanced following the procedure outlined in the manual. Each grid was surveyed by walking the gradiometer in a one-metre zigzag acquisition pattern, which provided an effective line space of half a metre. Twenty grid of 20 x 20 m each was completed, providing a total survey area of 80m by 100m (Figure 10). The corners of each survey grid were surveyed using RTK-GPS. The gradiometer data was collected roughly every 12.5 centimetres along each line, but this was affected by surface features such as dense shrubbery or holes in the ground. Non-metallic measuring tapes were used to mark the location of each grid and to guide the magnetometer operator. The magnetometer survey area overlaps with some of the ERT survey lines so that the two data sets can be compared after processing. Part of the survey was also conducted over the fence line, to compare the immediate subsurface on each side.

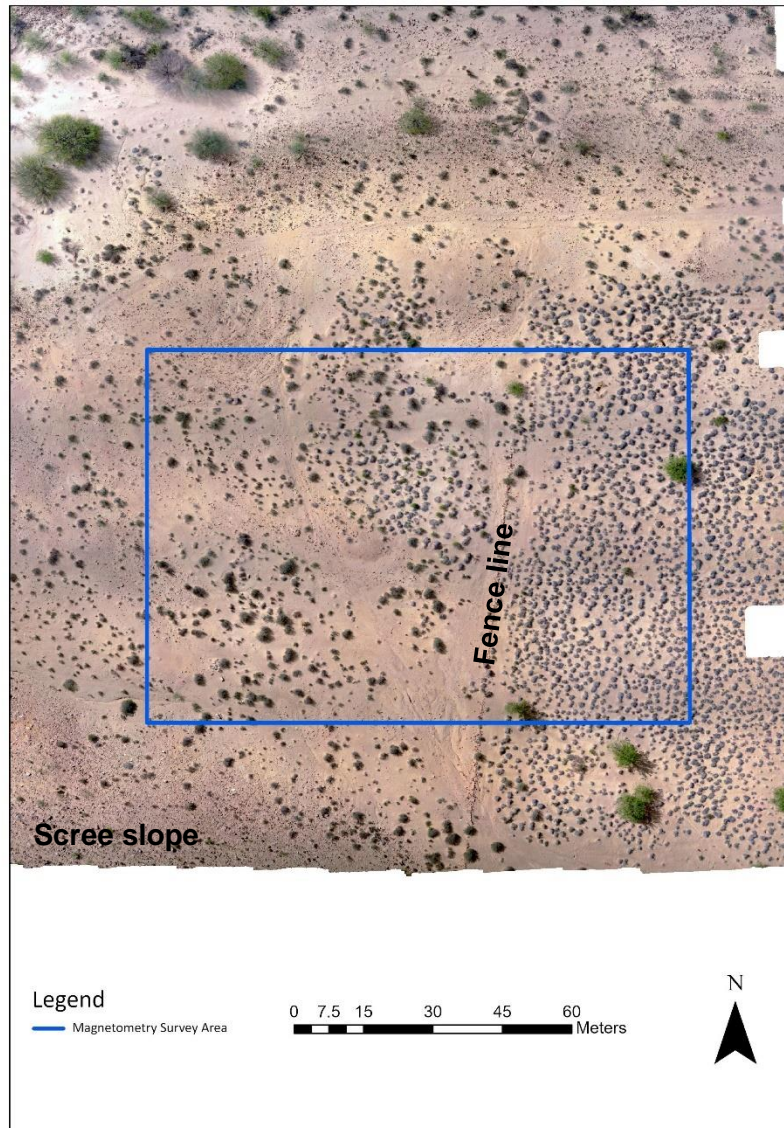


Figure 10: The magnetometry survey area.

Data Processing

All processing for the magnetometry data was completed via the Snuffler program. All twenty grids were imported into the software and then stitched together to make a single image. A test map was created to ensure the orientation and positioning of each grid was correct. Next, the data was destriped vertically and horizontally in Snuffler. This was conducted a few times, especially vertically, as the second half of the magnetometry results was significantly noisier than the first half. Next, the data

underwent a destagger and finally a interpolate filter to smooth it out and make the results more interpretable. The contrast display for the magnetometry survey was set to a $\pm 2.5\text{nT}$ image scale, to make sure the more subtle features were more viable. Finally, the map created in Snuffler was georectified in ArcGIS Pro using RTK points taken during fieldwork.

4.6 Magnetic Susceptibility

Theory

While magnetometry measures magnetic intensity, this magnetic method measures magnetic susceptibility (Schmidt 2007:4). This is done by the machine actively producing a magnetic field and measuring the propensity of a feature to be magnetised (Dalan and Banerjee 1998:6). Specifically in this survey, the magnetic susceptibility of stratigraphy within four trenches was tested. As discussed above human occupation and activities within an area can increase the magnetic susceptibility of soil. This allows for areas of burning to be detected where high magnetic susceptibility is detected within the stratigraphy, it may be a part of a paleosol where prehistoric fires burned (Dalan and Banerjee 1998:16; Maki et al. 2006:208). This can assist in locating areas or layers of a site where archaeology is more likely to be found and further knowledge about a site, its stratigraphy, and site formation (Dalan and Banerjee 1998:16). An example of this type of work has been conducted at Pinnacle Point 13B within the Western Cape of South Africa, where it was used to study spatial patterning (Herries and Fisher 2010:308–309). Other examples within South Africa include Grand Canyon Rockshelter, Rose Cottage Cave, Molony's Kloof, and Sibudu Cave (Herries 2009:237–238).

Instrumentation

The magnetic susceptibility of the different sedimentary layers in the subsurface was measured using a Bartington MS3 with an MS2K sensor. This is a lightweight and compact meter that can measure a range of soils, rocks, powders, and liquids, and has a measurement range of 26 SI (Bartington b:4). Bartington provides a variety of sensors for the MS3, each with a specific purpose (Bartington c:9) The probe used for this magnetic susceptibility survey was the MS2K High Stability Surface Scanning Sensor. The MS2K is a field survey sensor best suited for "highly repeatable measurements of the volume magnetic susceptibility of moderately smooth surfaces (Bartington c:51)." The depth of response for the MS2K is quite shallow, being reduced to 50% at 3mm depth and down to 10% at 8mm (Bartington c:52).

Data Collection

Magnetic susceptibility tests were utilised to identify paleosols and hearth features within the subsurface and assist in characterising the stratigraphy when combined with the ERT data. Dr Alex Mackay's team dug eleven trenches at KH1, which provided access to stratigraphy in parts of the site. Magnetic susceptibility measurements were taken in four of these pits, measured every 2 centimetres down one side of each trench, with a calibration measurement taken in the air every 10 samples to prevent instrument drift. The RTK was used to record the point where each magnetic susceptibility test was conducted (Figure 15). In conjunction with the magnetic susceptibility test, a sediment sample was taken at each data collection location. These samples were taken back to a laboratory and a sedimentary

classification will be conducted by Dr Brian Jones. This classification combined with the susceptibility test will provide greater knowledge of the stratigraphy of KH1 and will help in understanding and characterising the ERT results.

Trench 1 was dug near the beginning of Line 2, directly on top of a mound feature. Trench 5 was located near the first trench, but just off of the mound features. The location of Trench 6 was at the southern end of Line 1, on the edge of the scree slope. Finally, Trench 10 was the only trench tested that was located on the eastern side of the fence where the modern sediment is more common.

Table 3: Information on the trenches where magnetic susceptibility tests were conducted.

Trench	Max Depth (m)	Description
Trench 1	2.4	Very homogenous with silt and fine-grained sand that is very well sorted and rounded.
Trench 5	1.8	Roughly 5cm veil of modern unconsolidated sand. Under this, the sediment is fine-grained sand with some silt and is well sorted and rounded. At 90 cm the sediment becomes more indurated. Artefact horizon at 1m depth.
Trench 6	1.7	Much more clay-rich than the rest of the site. Includes discrete light-coloured bands which are very clay-rich.
Trench 10	2.15	Unconsolidated sand to 30cm. Less consolidated from 30cm to 60cm. Artefact horizon at 60cm depth. 60cm to 2.15m fine-grained sand with silt and well sorted and rounded.



Figure 11: Trench 1.



Figure 12: Trench 5.

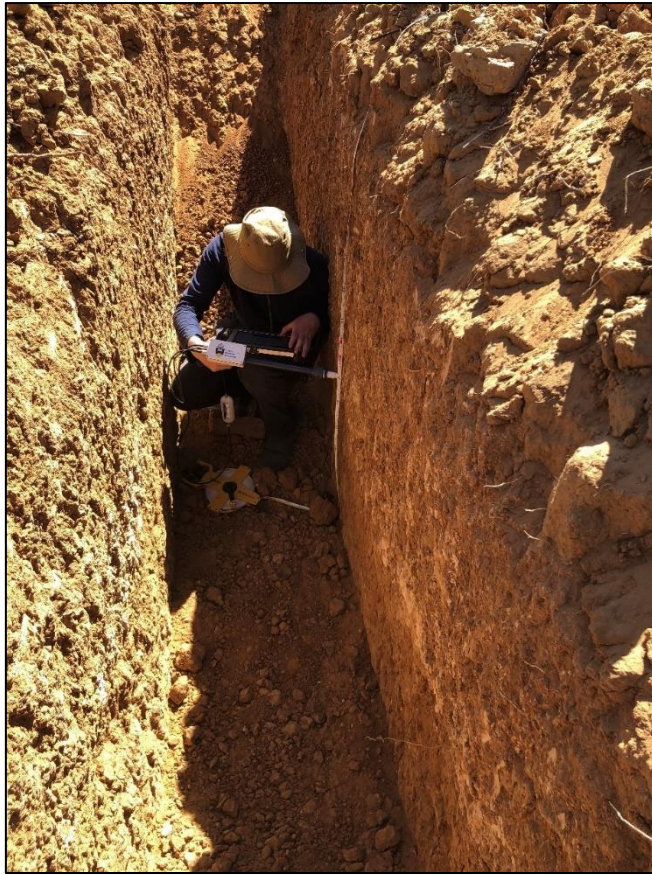


Figure 13: Trench 6.



Figure 14: Trench 10.

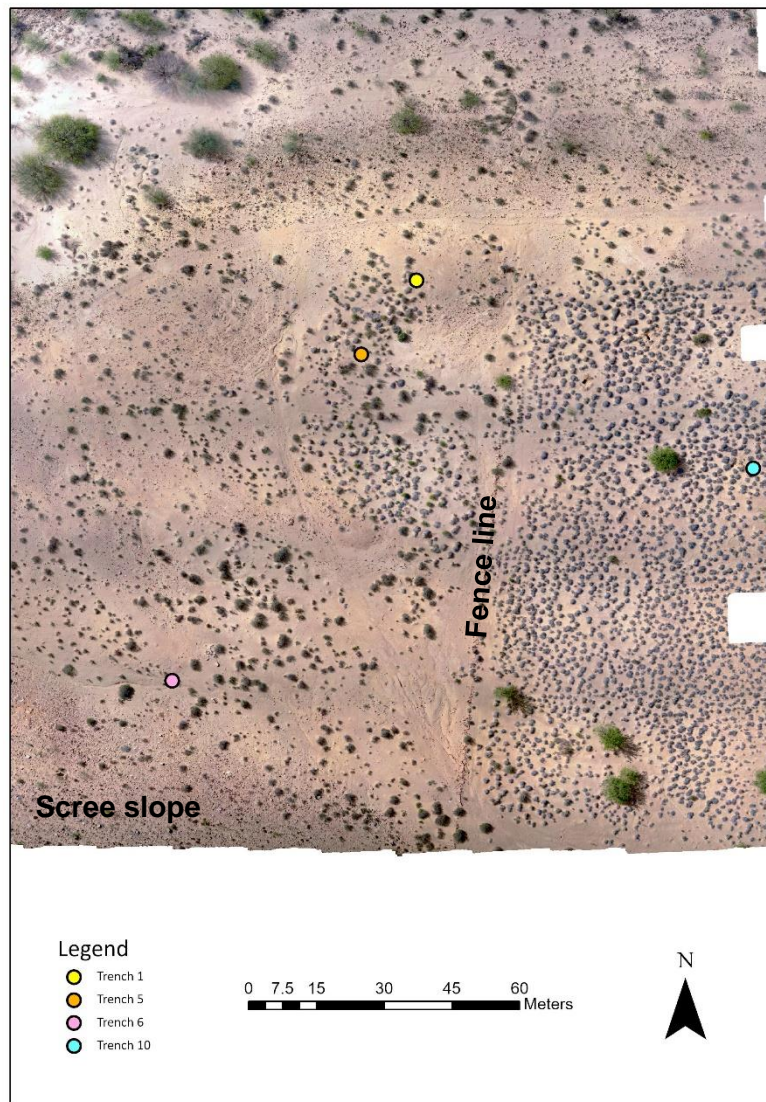


Figure 15: Location of the trenches where magnetic susceptibility tests were conducted.

Data Processing

The drift corrected data from the four magnetic susceptibility tests was downloaded and then opened in Microsoft Excel. An XY scatter plot with smooth lines was created to display the data.

5 Results

This chapter will discuss the results of the site survey and geophysical survey at KH1.

5.1 Site Survey

A survey of KH1 was conducted on the first day of fieldwork. The goal of this survey was to better understand the geology and archaeology of the site and to determine where the geophysical survey should be conducted.

Geology

Five stratigraphic units were identified during this survey. These are units are: modern unconsolidated aeolian sediment; semi consolidated aeolian sediment; sand and silt-sized fluvial sediment; cobble sized fluvial sediment; and the scree slope (Figure 16). The two fluvial sediment units are the most common units covering KH1, with the modern unconsolidated unit overlaying the semi consolidated unit in a thin veneer roughly less than a metre deep. Much of the modern aeolian unit has been eroded on the western side of the fence line, however, on the eastern side of the fence, most of this modern unit is still intact. The sand and silt-sized fluvial sediment is located on the northwestern side of KH1, in the riverbed of the Doring River. The cobble sized fluvial sediment is found on the northern side of the site, near the bank of the Doring River, and is likely a bolder bar that was created by the accumulation of sediment by the river. Finally, the scree slope is located on the southern edge of the site, partially draping over the site, and likely deposited by cliffs located south of KH1.

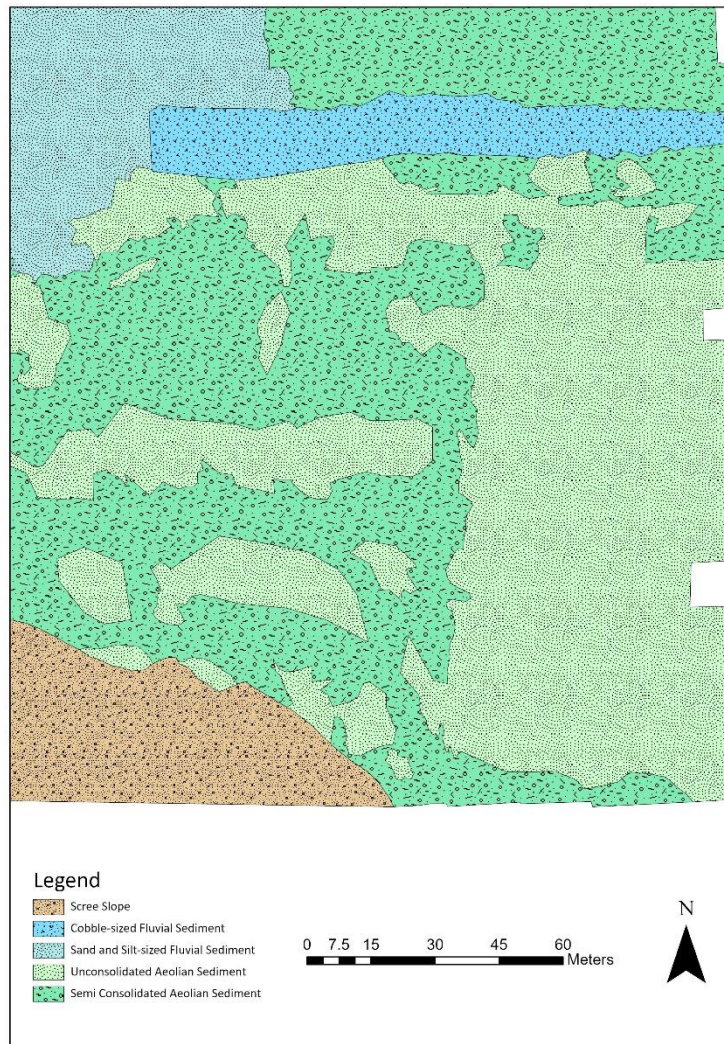


Figure 16: Geological map of KH1.

Table 4: Description of the geological units of KH1.

Geological Unit	Description
Scree Slope	Poorly rounded, angular rocks originating from the southern cliff.
Cobble-sized Fluvial Sediment	River rounded rocks with thin areas of sand-sized sediment.
Sand and Silt-sized Fluvial Sediment	A thin layer, less than a metre, of unconsolidated river sand and silt-sized sediment, overlying rounded cobbles.
Unconsolidated Aeolian Sediment	A thin veneer of modern unconsolidated sand-sized sediment, with very few rocks. Plenty of bush vegetation.
Semi consolidated Aeolian Sediment	Semi consolidated sediment with quite a few rocks on the surface. Evidence of carbonate material. Associated with the bifacial cluster.

5.2 Electrical Resistivity Tomography Results

5.2.1 Line 1

This line takes place on the western side of the site, starting in the fluvial sediment of the riverbed for the first roughly 16 metres, and then entering the aeolian sediment. It runs over the bar feature and westernmost mound before finishing before the scree slope begins.

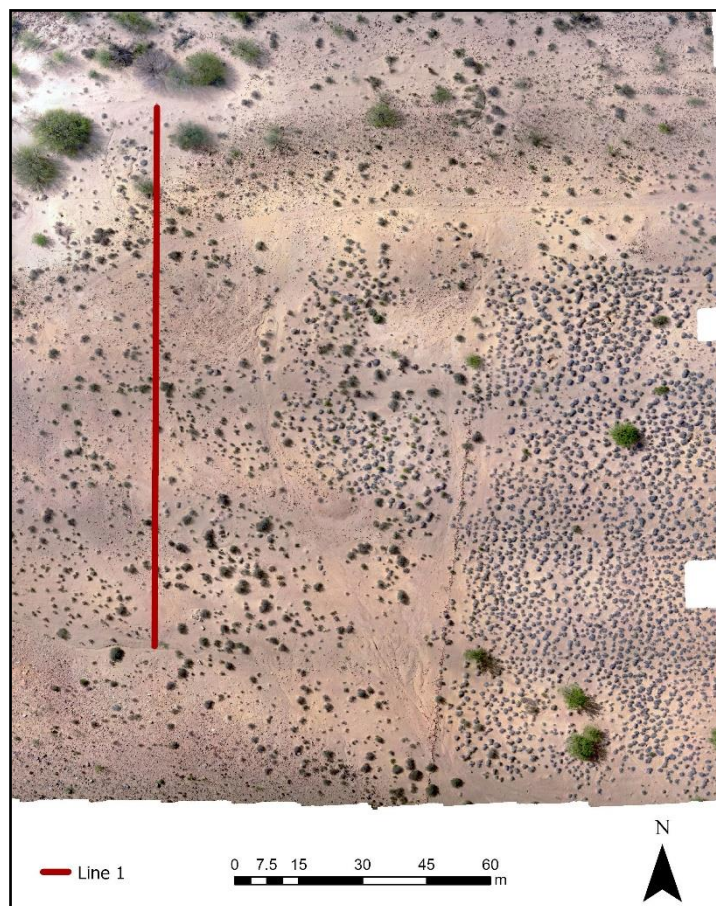


Figure 17: The location of Line 1.

Wenner Array

KF1 Line 1 All Rollis Wenner

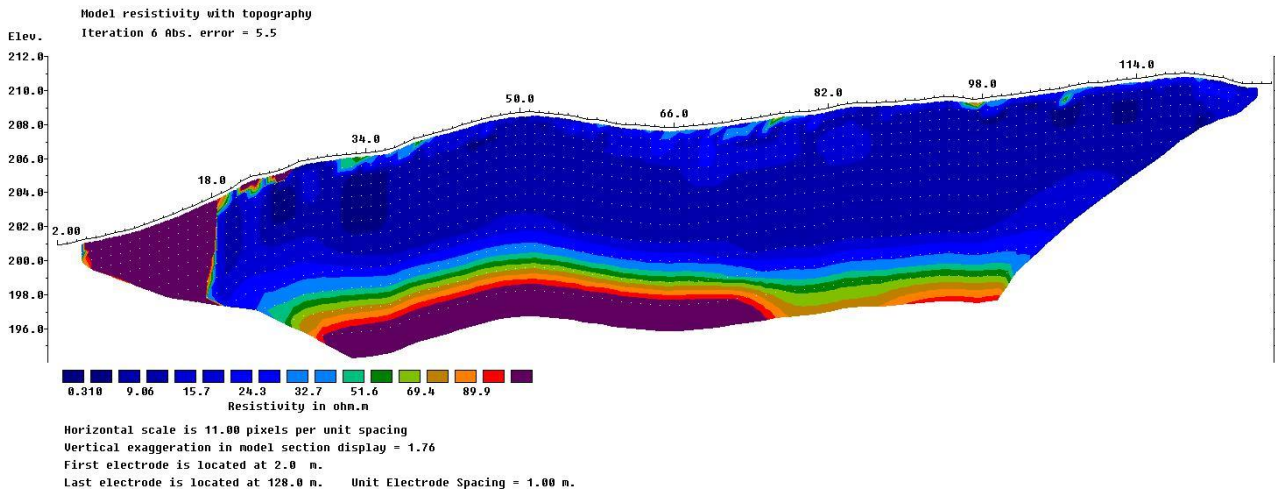


Figure 18: Wenner array of Line 1

From the start of the line until around the 18th electrode there is a large area of high resistivity material, from 89.9 to 1,986.8 $\Omega\cdot\text{m}$, that correlates with the presence of cobble-sized fluvial sediment on the surface. After electrode 18 there is a much smaller, shallow area of high resistivity sediment. From electrode 26 to between 31 and 32 is a flatter section with low resistivity, 0.310 to roughly 40 $\Omega\cdot\text{m}$, that corresponds with the archaeological surface of KH1, the semi consolidated aeolian unit. This is the largest and most widely distributed unit within the subsurface of this resistivity section. Between electrodes 31 to 35 and 36 to 41 there are examples of small patches of higher resistivity, between 40 to 60 $\Omega\cdot\text{m}$, occurring on the surface of the site. These patches also occur at the surface beneath electrodes 58, 63, 65-68, 70-79, 96-100, 106-109, 112-114, and 120. Apart from these surface patches, the subsurface is very homogeneous until a large, highly resistive unit begins between the elevations of 201 and 198. This unit measures approximately 40 $\Omega\cdot\text{m}$ towards the top and gets progressively more resistant as it gets deeper to roughly 152 $\Omega\cdot\text{m}$.

Dipole-dipole Array

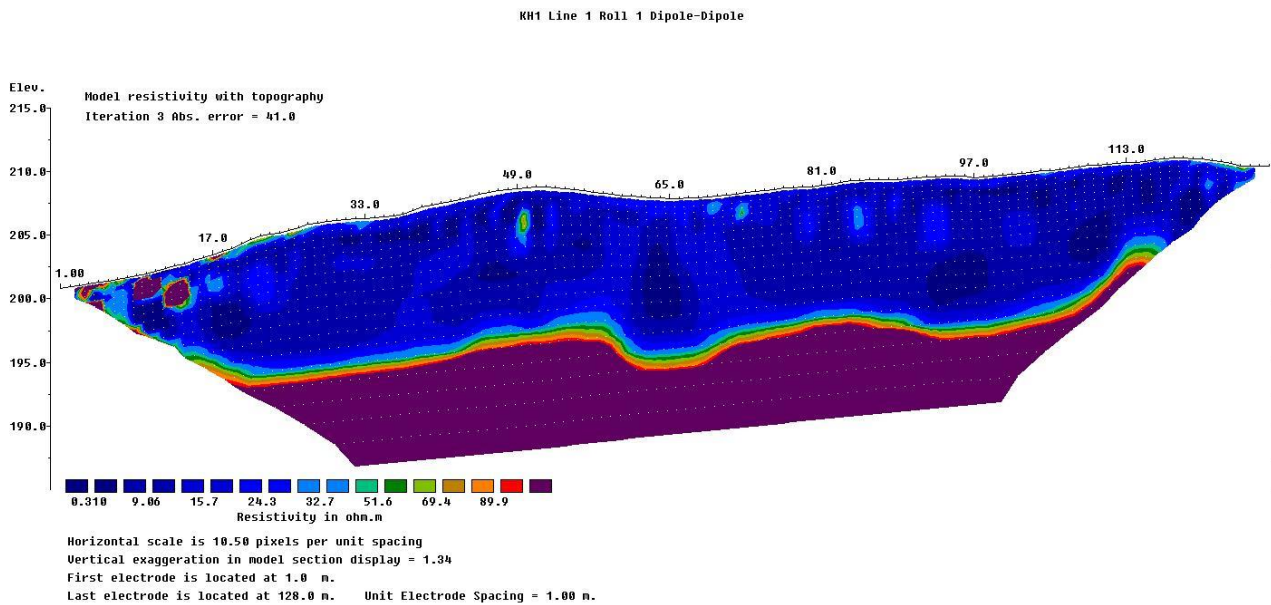


Figure 19: Dipole-dipole array of Line 1

This resistivity section begins with a very large variety of resistivity values up until electrode 19. In this section, there are multiple high resistivity units with measurements of 40+ $\Omega\cdot\text{m}$ on the surface and in the subsurface. These high resistivity units are generally quite small and shallow and are surrounded by a lower resistivity unit, measuring less than 40 $\Omega\cdot\text{m}$. This lower resistivity unit comprises the majority of the surface and subsurface within the resistivity section. At electrodes 20-23 and 25-27 there are surface units with a resistivity of roughly 40 to 60 $\Omega\cdot\text{m}$ and a depth of less than 1 metre. There is a similar feature at the end of the line at electrodes 123 to 126. Under electrodes 49 and 50, at an elevation of roughly 205 to 206, there is a small unit with a resistivity of 40 to 60 $\Omega\cdot\text{m}$, and a similar, but smaller, unit under electrodes 72 and 73 at an elevation of roughly 206. Starting at an elevation of around 197.5 to 195, a large, highly resistive unit measuring at 69.4+ $\Omega\cdot\text{m}$. This unit occupies the deepest portions of this resistivity section and rises slightly on the southern end of the line.

5.2.2 Line 2

This line was located in the centre of the site and like Line 1, it began in the riverbed of the Doring River. This line passed over the bar feature, a mound feature, and finished a few metres before the scree slope began.

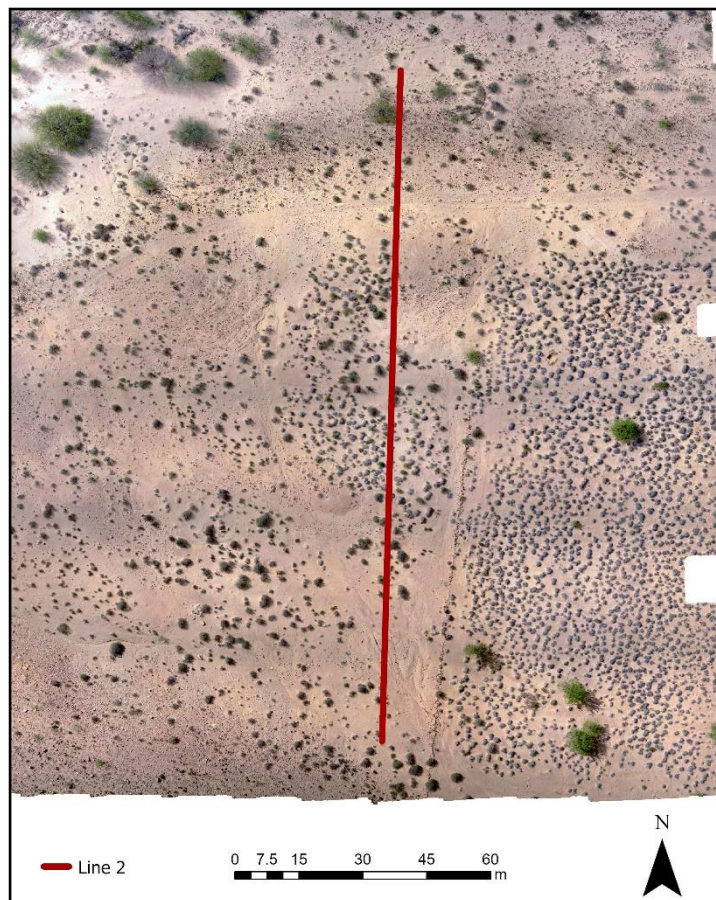


Figure 20: The location of Line 2.

Wenner Array

RH1 Line 2 All Rolls Wenner

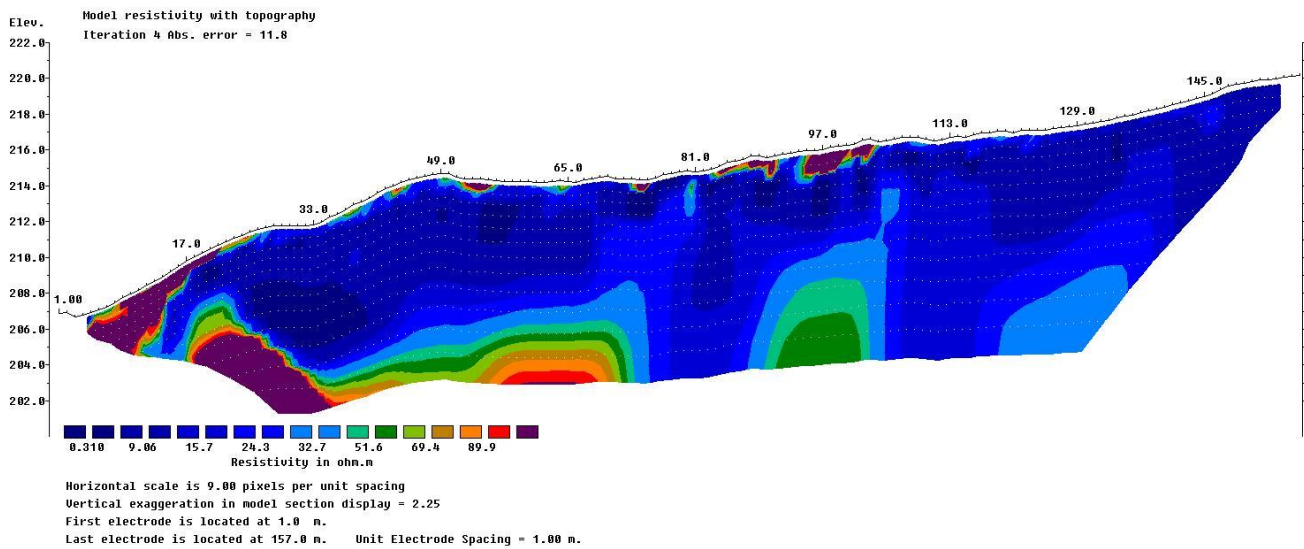


Figure 21: Wenner array of Line 2.

At the start of the line is a small unit of sediment with low resistivity, that is less than a metre deep. From electrodes 5 to 8, is a new unit with a resistivity value of roughly 50 to 60 $\Omega\cdot\text{m}$, which is also less than a metre deep. Electrodes 9 to 21 reveal a new unit with fairly high resistivity of 89.9+ $\Omega\cdot\text{m}$ that continues under the two previous units. Next, from 21 to 26 is another small unit, less than a metre deep, that has a resistivity property of around 40 to 80 $\Omega\cdot\text{m}$. A few more shallow areas of high resistivity appear on the surface around electrodes 34-39, 42-44, 49-56, 63-65, 73-75, 83-91, and 95-104. In the subsurface, there is a large unit of high resistivity towards the north side of the resistivity section. This unit begins at an elevation of 207 with a resistivity value of an estimated 40 $\Omega\cdot\text{m}$, but gradually increases the deep the unit is. This unit continues southward, towards the centre of the resistivity section, but here it portrays a lower resistivity value. Right under electrode 97, at an elevation of roughly 207 is a similar unit to the previous but with a lower value of around 40 to 60 $\Omega\cdot\text{m}$ and surrounded on its north and south side by a unit with much

lower resistivity. This final unit accounts for the rest of the subsurface and measures from 0.310 to roughly 40 $\Omega\cdot\text{m}$.

Dipole-dipole Array

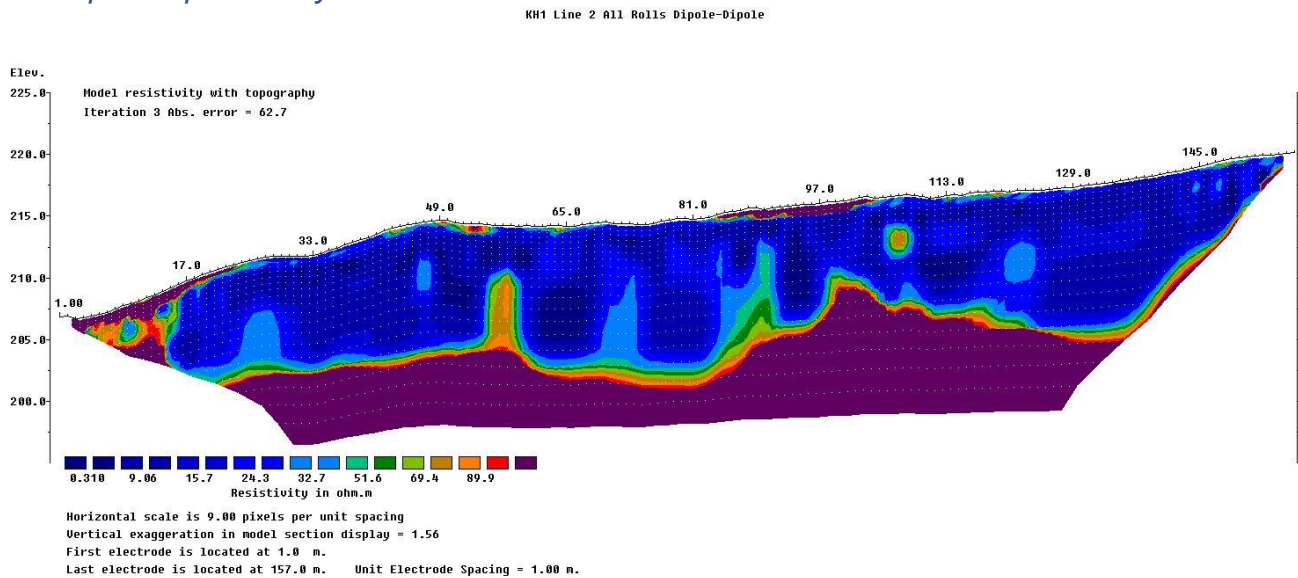


Figure 22: Dipole-dipole array of Line 2.

From electrodes 1 to 23 is a shallow, surface unit of highly resistive sediment. Under this unit, is an area that contains a wide range of resistivity values, from 9.06 to 89.9 $\Omega\cdot\text{m}$. Under this section is another highly resistive unit with values of 89.9+ $\Omega\cdot\text{m}$. On the surface, there are various units with resistivity values ranging from 40 to 89.9 $\Omega\cdot\text{m}$. The largest and most resistive of these units spans from electrode 84 to 104 only about 1 metre deep. A homogenous unit with values ranging from 0.310 to roughly 40 $\Omega\cdot\text{m}$ comprises the majority of the surface and subsurface of the resistivity section. Within this unit, under electrode 107, is a small unit with resistivity values of around 40 to 80 $\Omega\cdot\text{m}$. Finally, occupying the bottom third of the resistivity section is a large unit with resistivity values of 89.9+ $\Omega\cdot\text{m}$. This unit is topographically complex and rises on the southern side of the line, coming significantly close to the

surface of KH1. Some features protrude up from this unit, that possess high resistivity values, although lower than the bottom-most unit, ranging from an estimated 40 to 80 $\Omega\cdot\text{m}$.

5.2.3 Line 3

This was the final, and longest, ERT line conducted during the geophysical survey, consisting of five rolls with a total length of 192 metres. This was the only line to take place entirely within the eastern side of the fence line where erosion has been minimal, and the modern unconsolidated sediment is more widespread. Line 3 crosses a mound feature on the north side and the scree slope on the southern end.

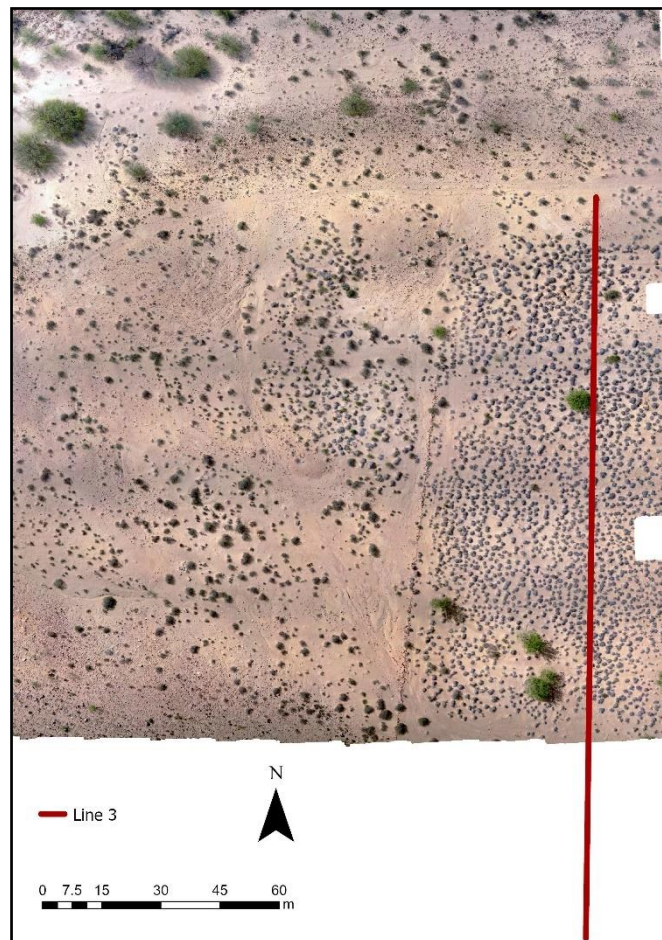


Figure 23: The location of Line 3.

Wenner Array

KH1 L3 All Rolls Wenner

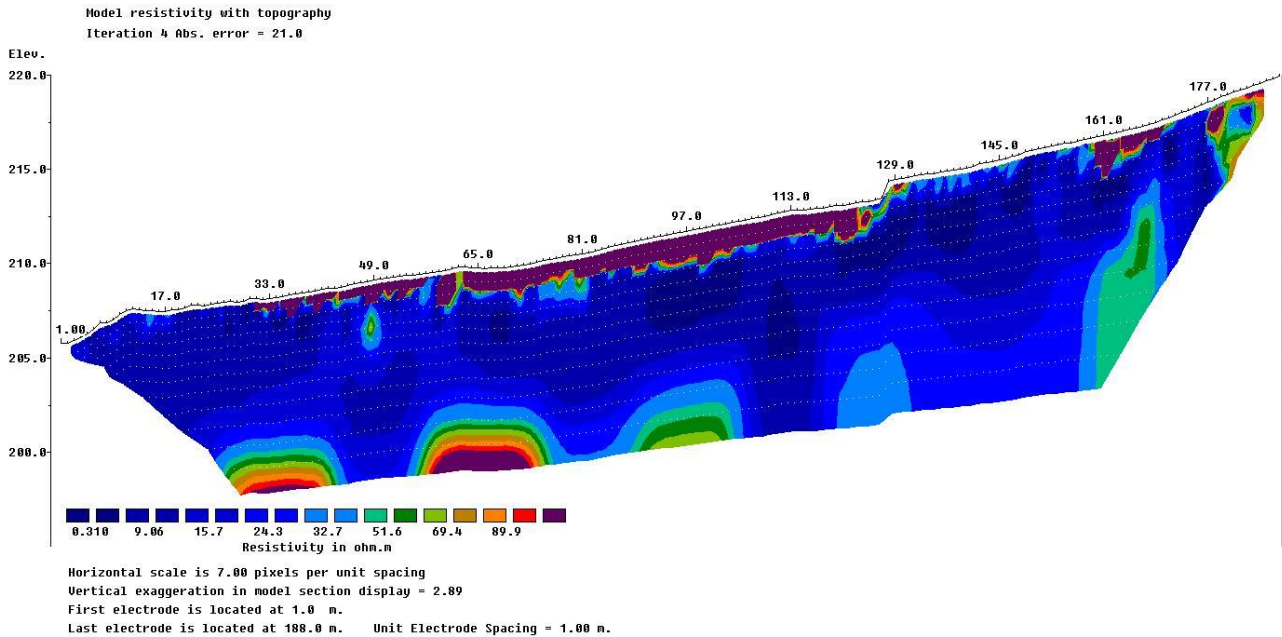


Figure 24: Wenner array of Line 3.

This resistivity section is dominated by a large, homogenous unit with resistivity values of 0.310 to around 40 $\Omega\cdot\text{m}$. Within this unit, under electrode 48, is a small feature with higher resistivity values, around 40 to 70 $\Omega\cdot\text{m}$. Almost two-thirds of the survey surface is made up of multiple units with high resistivity, all measuring above 40 $\Omega\cdot\text{m}$, but the majority above 89.9 $\Omega\cdot\text{m}$. These units generally do not extend very far into the subsurface and the majority are situated within the central section of the surface. There is a similar unit on the southern side of the line, between electrodes 159 to 171, that is separate from the previous unit. From electrode 177 to the end of the line, is a section of widely varying resistivity values, varying from 0.310 to above 89.9 $\Omega\cdot\text{m}$. Unlike previous resistivity sections, there is not a large, highly resistive unit at the bottom of this section. A few units are protruding up from below the survey

area which have a higher resistivity value than the majority of the subsurface, generally above 40 $\Omega\cdot\text{m}$.

Dipole-dipole Array

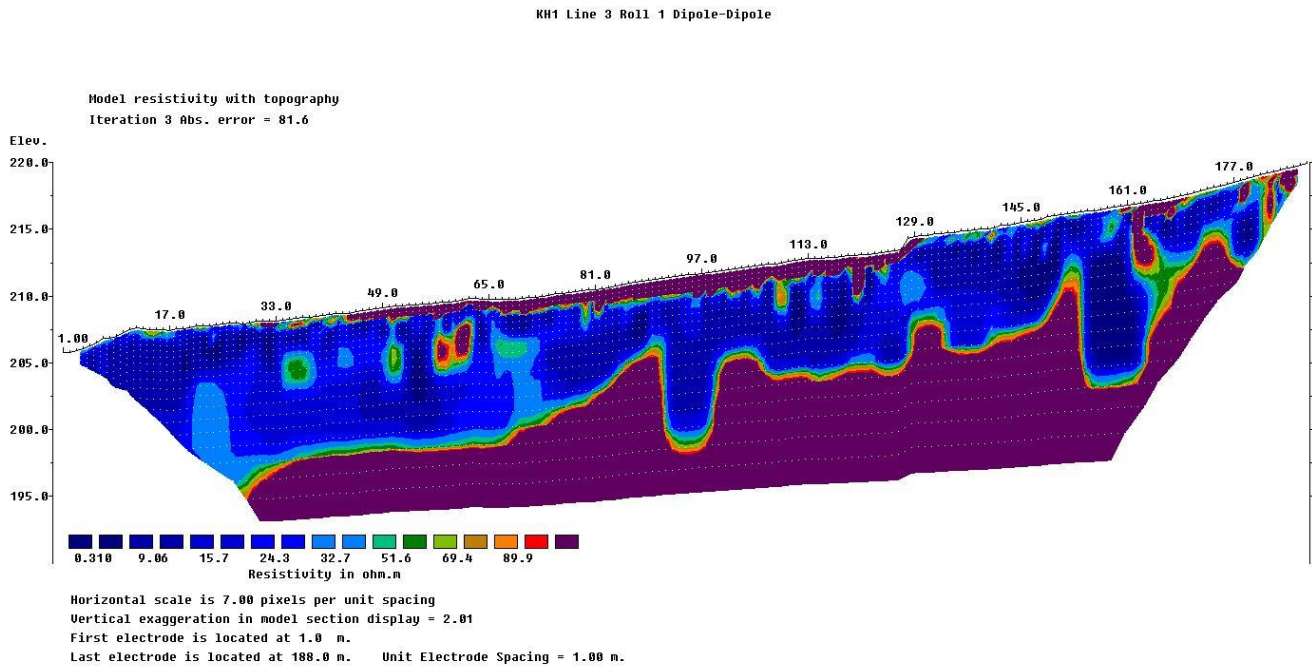


Figure 25: Dipole-dipole array of Line 3.

The majority of the subsurface in this resistivity section is made up of units with high resistivity. A homogenous unit with resistivity values exceeding 89.9 $\Omega\cdot\text{m}$ occupies roughly half the surface but does not extend far into the subsurface. From electrodes 31 to 33 and 160 to 170 are smaller units with similar resistivity values to the large surface unit. There are surface units, generally smaller than the previous units, with values ranging from roughly 40 to 80 $\Omega\cdot\text{m}$. From electrode 179 to 186, is an area of highly varying resistivity values, ranging from the lowest value of 0.310 $\Omega\cdot\text{m}$ to exceeding 89.9 $\Omega\cdot\text{m}$. The middle of the resistivity section is primarily made up of a homogenous unit with resistivity values ranging from 0.310 to 40 $\Omega\cdot\text{m}$. within the northern side of this unit there are several anomalies with higher values, some of

which exceed 89.9 $\Omega\cdot\text{m}$. Finally, unlike the previous array of the same line, there is a substantial unit of highly resistive material at the bottom of the resistivity section.

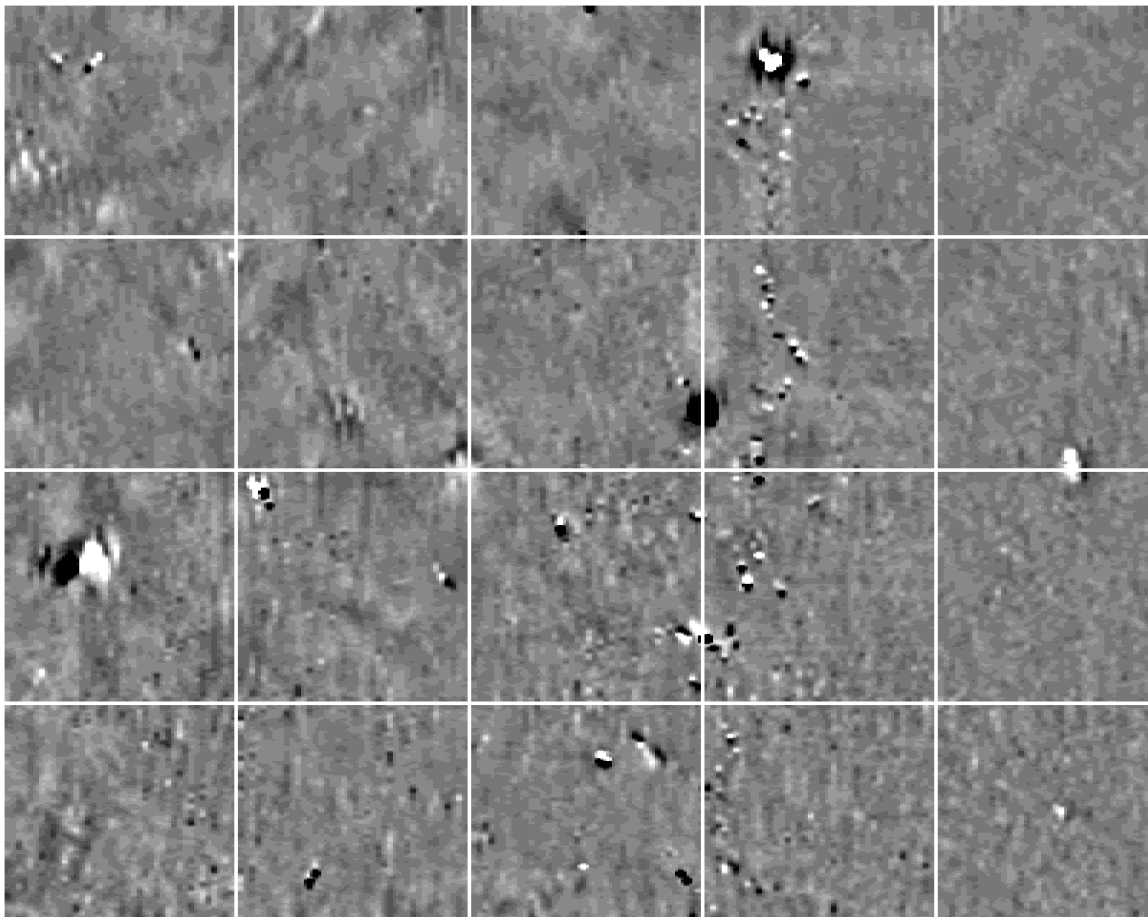
This unit is topographically complex with the deepest part located around elevation 195, and the highest point almost reaching elevation 215. Under electrode 164, this lower unit connects to a surface unit with similar resistivity values through a section with lower values of 40 to 80 $\Omega\cdot\text{m}$.

5.2.4 Summary

The results of the ERT survey lines are all comparable, with a few similar features showing up across multiple lines. Lines 1 and 2, especially the Wenner Arrays, both display a large, highly resistive feature at the beginning of the lines. All three lines have evidence of a very large stratigraphic unit that makes up the majority of the subsurface and consists of resistivity values of 0.310 to around 40 $\Omega\cdot\text{m}$, which is characteristic of clay-rich sediment. This unit also makes up a majority of the surface within the lines and is roughly 8m deep. All of the lines also display another surface unit, with a high resistivity of 89.9+ $\Omega\cdot\text{m}$, that is generally less than a metre thick. On Lines 1 and 2, this unit only makes up roughly a third of the surface, however, on Line 3 this feature is much more prominent, occupying over half the surface area and extending deeper into the subsurface. Each of the Dipole-dipole Arrays has a highly resistive, topographically complex unit occupying the bottom of the resistivity section, under the large, less resistive unit.

5.3 Magnetometer Results

The magnetometry survey consisted of a total of twenty 20 m by 20 m grids, for a total survey area of 80m by 100m in the centre of KH1. Each grid was surveyed in a 1m zig-zag pattern with readings taken roughly every 12.5 cm.



1	2	3	4	5
6	7	8	9	10
11	12	13	14	15
16	17	18	19	20



Figure 26: Results of the 20 x 20 m magnetometry grids combined into one map. The number of each grid is referenced underneath.

The results from the magnetometry survey show that there are three areas of relatively high magnetic intensity within the survey area. The first of these is a large anomaly in the top left section of grid 4 (-36.91 to 3.82 nT), while the second appears across grids 8 and 9 (-0.4 to 27.52 nT). The third and largest of these magnetically intense anomalies is located within grid 11 with values of -10.69 to 14.38 nT. There are many smaller areas of high magnetic intensity across the survey area, however, the majority of these are located across the left sides of grids 4, 9, 14 and 19 and string together forming a rough line with values of -16.83 to 10.24 nT. To the right of these anomalies, in grids 5, 10, 15 and 20 the magnetic intensity is relatively uniform, apart from the anomalies already mentioned, with values of around -0.62 to 0.63 nT. This contrasts with the other side of the magnetometry survey where in grids 1-3, 6-8, 11-13 and 16-18 the results fluctuate significantly more. Within these grids, especially towards the top of the survey, are many subtle anomalies. A few examples of these subtle anomalies occur at the bottom centre of grid 3 (-0.44 to 1 nT), the middle of grid 12 (-0.94 to 0.78 nT), and between grids 1, 2, 6 and 7 (-0.91 to 0.72 nT). Finally, the bottom half of the survey area, especially the bottom left, is noticeably more grainy and less smooth than the rest of the results.

5.4 Magnetic Susceptibility Results

5.4.1 Trench 1

The magnetic susceptibility test on Trench 1 was conducted on the west side of the pit with samples taken every 2 cm.

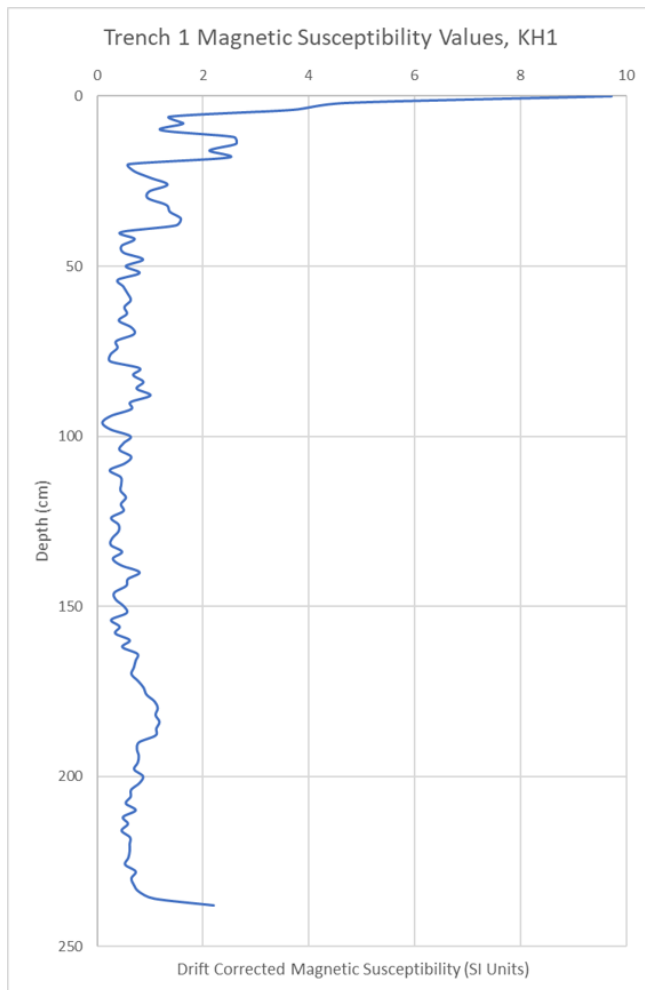


Figure 27: Magnetic susceptibility results from Trench 1 (left). The location of Trench 1 (right).

The magnetic susceptibility results display a reading of just under 10 SI at 0 depth. This is relatively high compared to the rest of the data but rapidly decreases, coming to around 1.7 SI at a depth of around 5cm. The magnetic susceptibility then rises again around 15 cm, where it peaks at approximately 2.3 SI. At 20 cm the susceptibility lowers again, dropping to roughly 0.5 SI. Between an estimated 25 cm and 40 cm of depth, the SI ranges from 1 to 1.5 SI. After this depth the magnetic susceptibility is relatively lower and steady, ranging from just over 1 SI to almost 0 SI at 96 cm. At the deepest part of the test, 2.4 m, there is a rise in SI again to just over 2.1.

5.4.2 Trench 5

The east side of Trench 5 was used for the magnetic susceptibility test and measurements were taken at 2cm increments.

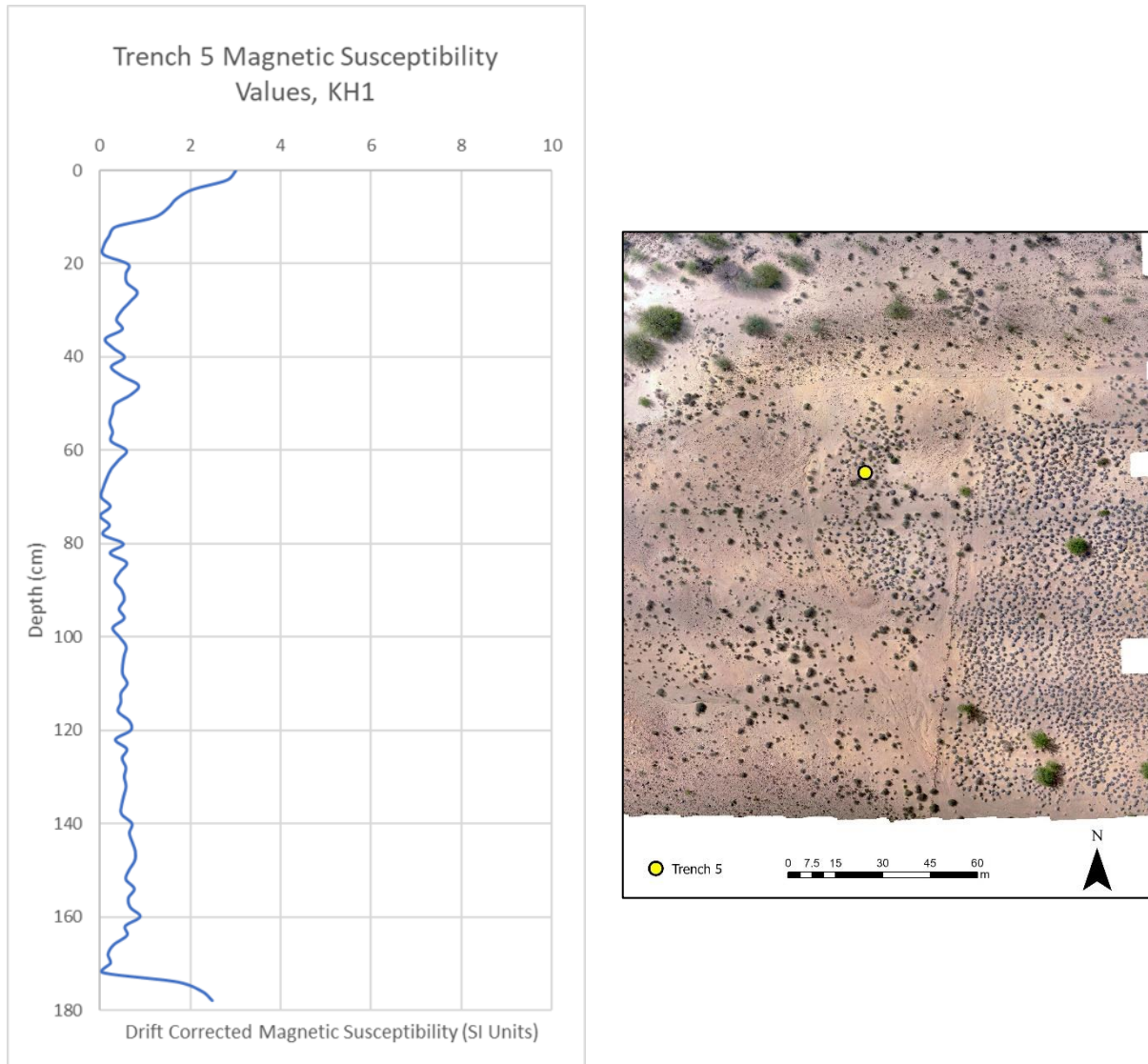


Figure 28: Magnetic susceptibility results from Trench 5 (left). The location of Trench 5 (right).

The magnetic susceptibility for this trench starts at roughly 3 SI but decreases until at a depth of 18cm where the susceptibility is 0 SI. Between 20 and 25 cm the susceptibility rises slightly to around 0.75 SI. The magnetic susceptibility around 45 cm peaks to an estimated 0.75 SI but quickly decreases as the depth increases. The

rest of the trench is rather consistent with no large variations in the magnetics susceptibility results. However, after 160 cm the susceptibility lowers decreases significantly until at 170cm it reaches 0 and then after rises suddenly to 2.5 SI.

5.4.3 Trench 6

The magnetic susceptibility test for Trench 6 was conducted on the east side, with measurements taken every 2cm.

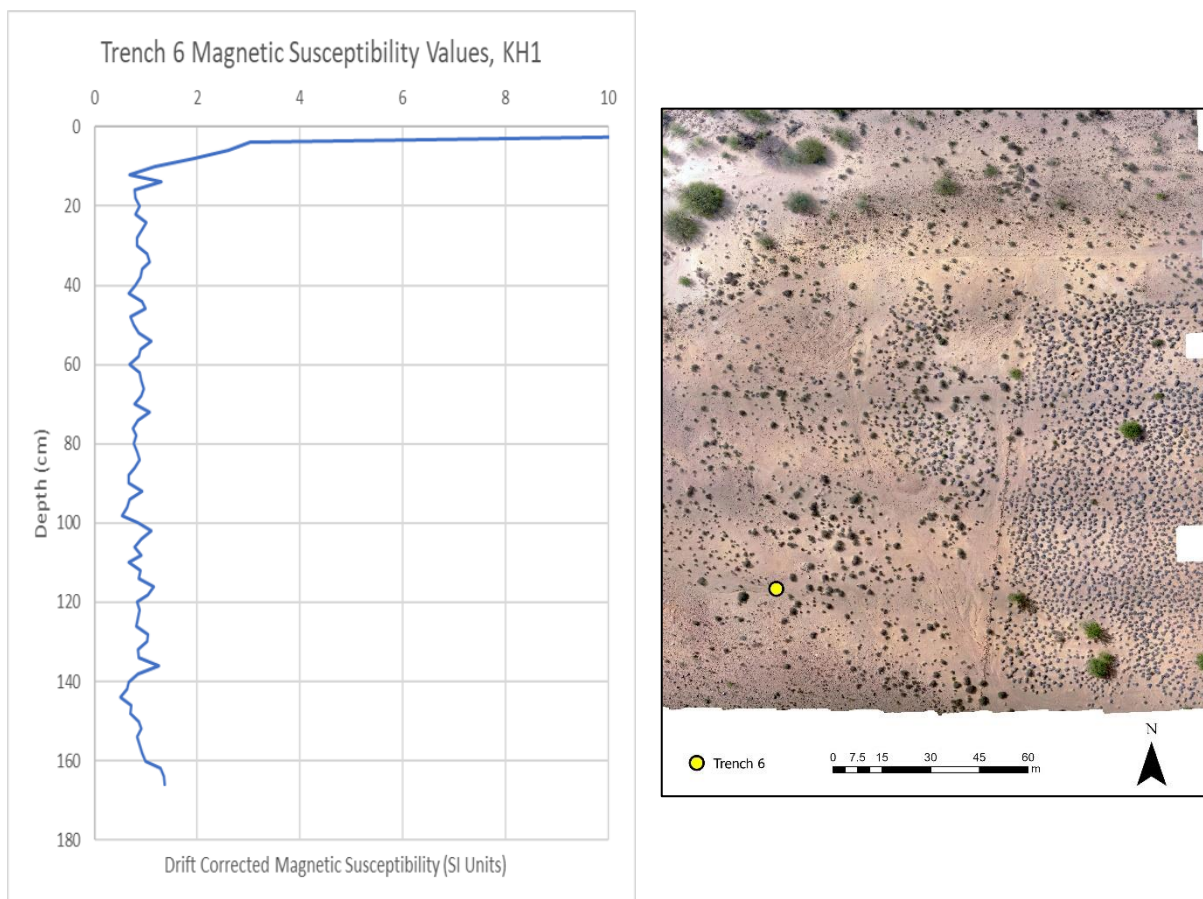


Figure 29: Magnetic susceptibility results from Trench 6 (left). The location of Trench 6 (right).

The magnetic susceptibility at the surface of Trench 6 is significantly higher than the rest of the pit. However, the susceptibility quickly drops to 3 SI at roughly 5cm depth and 1 SI at around 15cm. There is a slight increase in magnetic susceptibility

between 15 and 20 cm, but not a substantial increase. From 20 cm to around 140 cm, the susceptibility of Trench 6 is relatively stable, only fluctuating slightly from an estimated 0.5 SI to 1 SI. After 140 cm the magnetic susceptibility drops to under 0.5 SI, the lowest results from Trench 6. From this point, the results steadily increase until the bottom of the trench, reaching a maximum value of 1.5 SI.

5.4.4 Trench 10

The final magnetic susceptibility test was conducted on the east side of Trench 10 and measurements were taken at 2 cm increments.

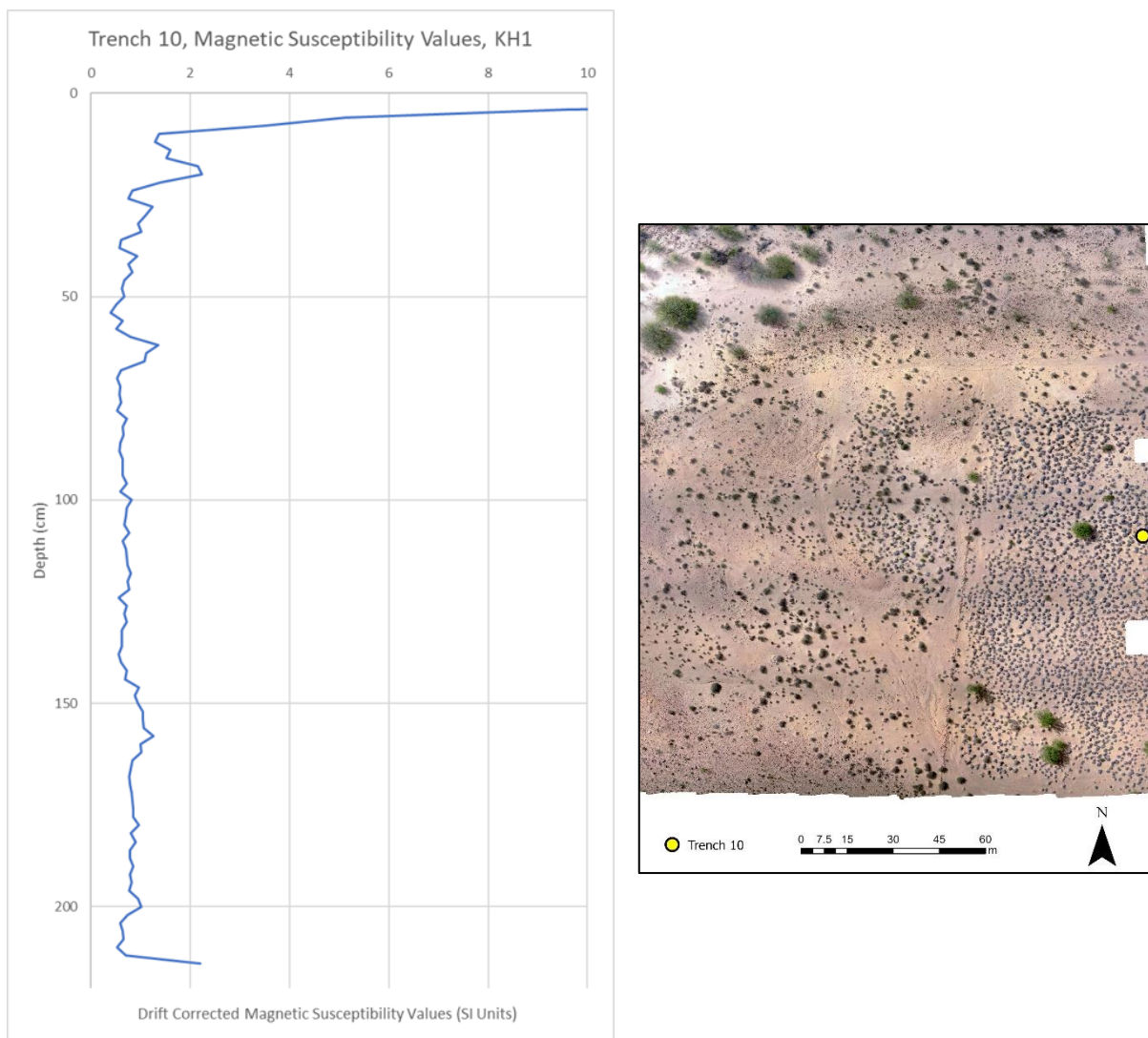


Figure 30: Magnetic susceptibility results from Trench 10 (left). The location of Trench 10 (right).

The beginning of this magnetic susceptibility test measures significantly higher than the rest of the results. The SI quickly decreases to 1.5 SI around 10 cm, then quickly rises to just past 2 SI at roughly 20 cm. Although, from this point until 55 cm, there is a downward trend in magnetic susceptibility results for Trench 10, albeit with a couple of slight increases as well. There is a small rise at the 60 cm mark, where the susceptibility increases to just past 1 SI. From around 70 cm to 140 cm, the magnetic susceptibility results are very stable, with very minimal changes. There is another slight rise around 150 cm of depth and then a very significant increase right at the bottom of the trench, where susceptibility is 2+ SI.

5.4.5 Summary

The magnetic susceptibility test results from each trench are comparable to one another. All start with a significantly high susceptibility at the beginning of the test with readings of 10 SI and higher. Trench 5, however, is slightly different with only a 3 SI reading at the start of the test, which while much lower than the other lines at the same point, is still much higher than the rest of the results from Trench 5. All of the trenches also display a small increase in magnetic susceptibility around the 15cm to 20 cm marks. After this point, the majority of the test results are relatively stable, with no major increases or decreases in magnetic susceptibility. This changes at the bottom of each trench, where an increase in magnetic susceptibility appears. This occurs at the bottom of each trench even though they all end at varying depths. Trench 6 does have an increased magnetic susceptibility towards the bottom of the trench, however, it is much lower than the results from the other trenches. There is an anomaly of high magnetic susceptibility in Trench 10 at a depth of 60 cm, that does not appear on the other tests.

6 Discussion

The main aim of this project was to determine what a geophysical survey could reveal about the archaeology and depositional history of an open-air site in a southern African context. To further this goal, a geophysical survey was conducted at KH1, the results of which would be used to answer the research questions proposed by this project.

This chapter will discuss the results of the three geophysical survey methods utilised, electrical resistivity tomography (ERT), magnetometry, and magnetic susceptibility, and how the findings of these methods answer the primary and secondary research questions.

The only excavations that have occurred at KH1 at this time are eleven trenches, the deepest of which is roughly 2.3 m. Thus, ground proofing for the results of the geophysical survey is not currently possible for much of the site due to the vast surface area and deep stratigraphy. Therefore, this discussion will largely be interpretations based on the results of each geophysical method and the geology, topography, and archaeology of the site.

6.1 Electrical Resistivity Tomography

Stratigraphy

The results of the ERT survey identified four stratigraphic units within the subsurface of KH1 (Figure 31). The first and smallest of these is the unconsolidated unit of aeolian sediment on the surface of the site. In the ERT models, this unit appears as a high resistivity unit, with values of 90 to 4,524 $\Omega\cdot\text{m}$. The unconsolidated aeolian unit is revealed to be relatively thin, with a max depth of about one metre, however,

in Line 3 this unit encompasses over two-thirds of the surface area and extends roughly two metres into the subsurface. This is likely due to the location of Line 3 on the eastern side of the fence line where the impact of erosion has been minimal when compared to the western side of KH1.

The second stratigraphic unit consists of semi consolidated aeolian sediment. This is the largest of the four units and has a relatively low resistivity value of 0.3 to ~40 $\Omega\cdot\text{m}$, which suggests that it is clay-rich sediment. The semi consolidated unit extends across much of the surface area of the site and has a thickness of between six to eight metres. The cluster of bifacial artefacts on the surface of KH1 is located within this unit and erosional effects in this area likely caused the cluster to surface. The ERT data revealed that the unit is much thinner around the cluster when compared to the rest of the site, indicating that the bifacial point originated from deeper within the unit. This presents a problem for any future excavations of the site as the extensive geographic distribution of this unit makes it difficult to identify a specific area or depth where archaeological material may be present. However, the size of the semi consolidated unit also means that any archaeological material towards the bottom of this unit may be significantly older than the bifacial points discovered on the surface.

The next stratigraphic unit is the cobble sized fluvial sediment unit that makes up the boulder bar on the site. This unit appears on Lines 1 and 2, at the beginning of each line right next to the riverbank of the Doring River. This unit has been identified as the boulder bar due to its location on the lines and within the site, and due to its highly resistive nature of 45 to 2,364 $\Omega\cdot\text{m}$. The ERT survey revealed that the boulder bar does not continue laterally throughout the site, reaches a max depth of seven metres, and is about 13 metres wide.

The final unit identified in this ERT survey is the highly resistive unit located under the semi consolidated aeolian unit. This unit is the deepest unit and the only unit that does not outcrop in the surface area. Due to these characteristics and the highly resistive properties of the unit, 89.9 to 20,846 $\Omega\cdot\text{m}$, this is interpreted to be a consolidated unit with a lithology of siltstone that makes up the bedrock of the site. This top of this unit is topographically complex, especially in the dipole-dipole array of Line 3, likely due to the migration of Doring River palaeo-channels.

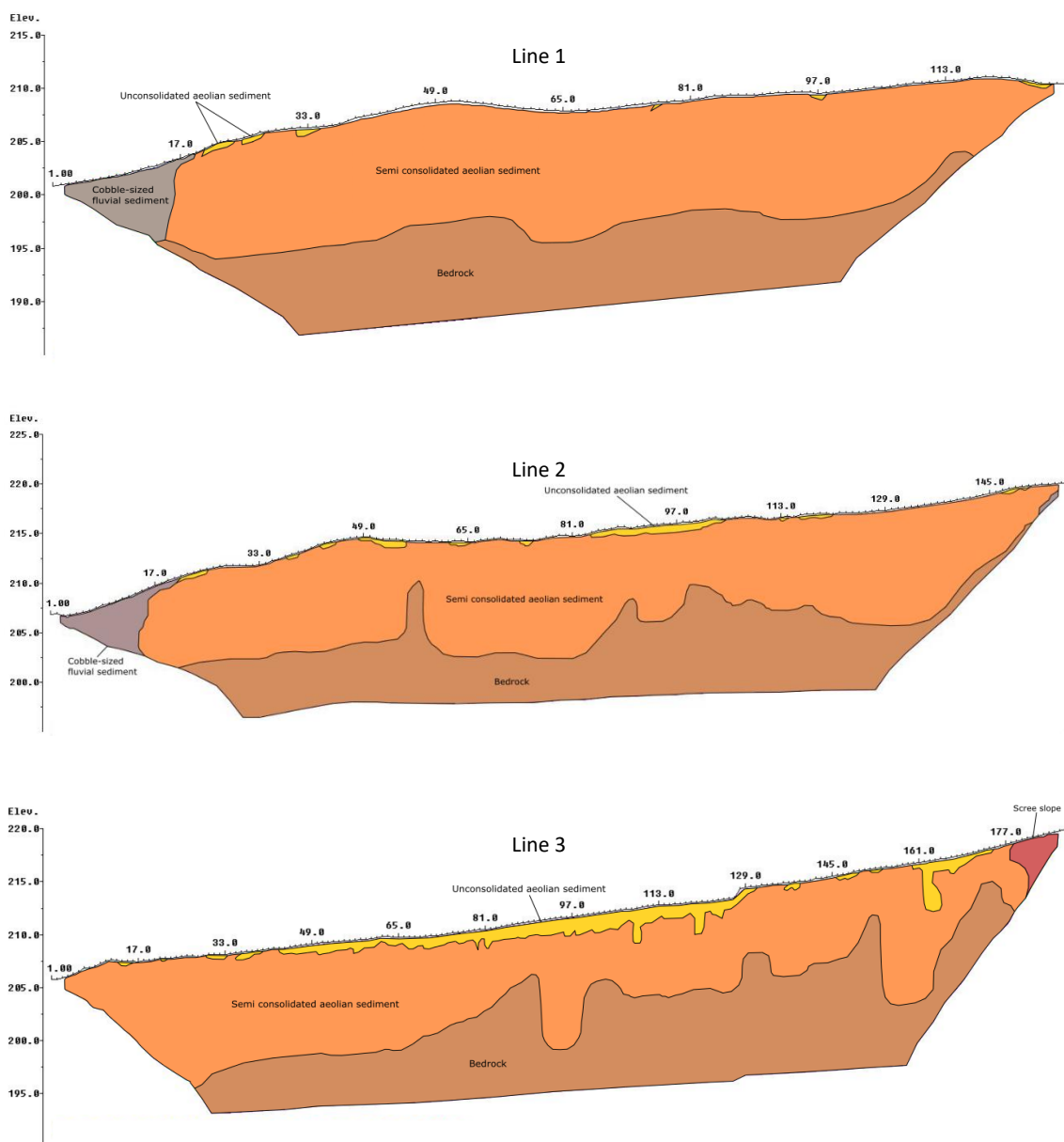


Figure 31: Interpretations of the stratigraphy of Line 1 (top), Line 2 (middle), and Line 3 (bottom) based on the ERT sections.

Anomalies

Several anomalies have been identified by the ERT survey, the most common of which are found within the semi consolidated aeolian sediment. These anomalies appear as small, highly resistive units making them easily identifiable as they contrast with the low resistivity of the semi consolidated unit. Examples can be seen in the dipole-dipole array of Line 1 under electrode 49, in the dipole-dipole array of Line 2 under electrode 107, in the Wenner array of Line 3 under electrode 49, and throughout the subsurface of the dipole-dipole array of the same line between electrodes 33 and 65 (Figure 32).

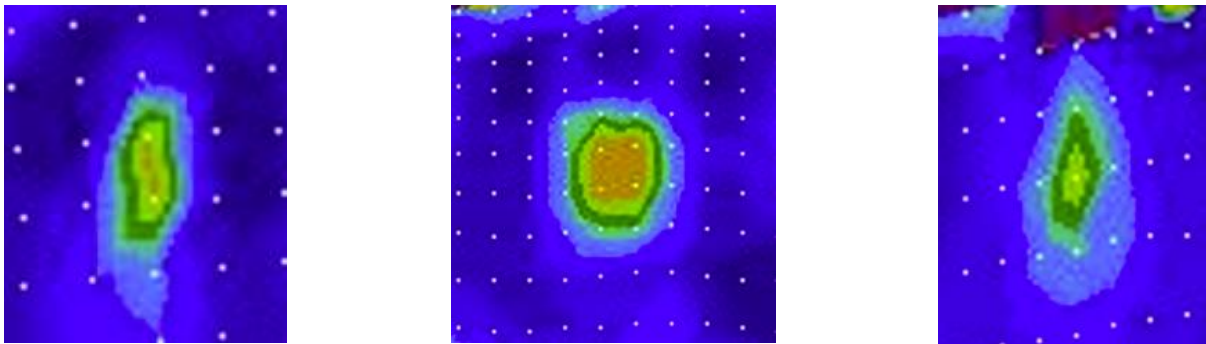


Figure 32: Examples of small, highly resistive anomalies in the dipole-dipole array of Line 1 (left), the dipole-dipole array of Line 2 (centre), and the Wenner array of Line 3 (right).

The majority of these anomalies are rounded and are generally one to three metres in length and two to three metres in height. The anomalies appear at different elevations within each line. The top of the anomaly in Line 1 is around an elevation of 205, while in Line 2 the anomaly begins at an elevation of around 217. Finally, in Line 3 the anomaly in the Wenner array begins at an elevation of roughly 207, however, the multiple anomalies in the dipole-dipole array begin at roughly the same elevation of 205. These anomalies are too large to be boulders and are more likely just discrete variations within the lithology of the semi consolidated unit.

Another anomaly appears at the end of Line 3 in both arrays, from electrode 177 to the end of the line. This feature has a large range of resistivity values from 0.310 $\Omega\cdot\text{m}$ to 89.9 $\Omega\cdot\text{m}$. This makes this feature one of the most varied in terms of resistivity properties. Due to the location of this feature at the end of Line 3, it has most likely been created by the scree slope. This would explain the range of resistivity values as the scree unit is poorly sorted and mixed and contains a wide variety of rock, sediment, and porosity.

The final anomaly appears within the dipole-dipole array of Line 2. In this model, it is evident that there are features that protrude up from the bedrock unit. The most prominent of these features is located under electrode 57 and begins around an elevation of 212. This specific feature has a relatively high resistivity value of between roughly 40 to 80 $\Omega\cdot\text{m}$ but is still lower than the resistivity of the bedrock unit. There is a similar feature in the same line under electrode 89, however, this feature has a much lower resistivity property of around 40 to 60 $\Omega\cdot\text{m}$. Finally, two more subtle features are extruding from the bedrock under electrode 27 and electrode 72, which are similar to the first two discussed but with a much lower resistivity value of around 40 $\Omega\cdot\text{m}$ and thus may be part of the semi consolidated unit. It is difficult to ascertain what these features may be, as they only appear on one line and within one array on that line. These features may represent a discrete change in the lithology of the bedrock and their shape may be due to the erosional effects of paleochannels.

6.2 Magnetometry

The anomalies in the magnetometry results can be characterised by strong anomalies, with values of -36.91 to 27.52 nT, and subtle anomalies, with values of -0.94 to 1 nT. The most prominent of the strong anomalies occur in the top of grid 4 and the top left section of grid 11. These anomalies display a very strong magnetic intensity that is suggestive of a large ferrous metal object. This is understandable as the location of these anomalies is the same as permanent survey markers placed on KH1 by Dr Mackay's team in earlier field seasons, which are made from ferrous metal surrounded by concrete.

The next most prominent anomalies are much smaller than those just discussed but are much more numerous in the survey area. These are very small anomalies of high magnetic intensity, the majority of which occur within grids 4, 9, 14, and 19. The anomalies in these grids form a rough north to south line, which is positioned in the same vicinity as the old fence line. As surveys of the site revealed metal on the remaining fence, these anomalies are interpreted as the remnants of the fence that have spread into the surrounding near-surface as the fence has decayed over time. Similar, anomalies can be seen throughout the survey area west of this fence anomaly, which is likely from modern metals found on the surface and in the near-surface, potentially originating from the fence.

As the primary goal of the magnetometry survey was to identify and locate hearths within the subsurface of KH1, the subtle anomalies are of the most interest to this project. Subtle anomalies can identify throughout the west side of the survey area, such as at the bottom of grid 3, in the middle of grid 12, and between grids 1, 2, 6 and 7. These anomalies have been interpreted as having been created by burning, due to the size and magnetic intensity of the anomalies. Thus, future excavations of

KH1 should consider these anomalies as areas of high archaeological potential due to the presence of hearths (Figure 33). These anomalies primarily occur in areas where considerable erosion has occurred and the semi consolidated sediment has been exposed, thus, the archaeology is likely located deeper in the site in the areas where erosion has been limited. Interestingly, these anomalies do not appear on the eastern side of the fence line. This is reasonable as the fence line has protected this side of the site from erosional effects, causing the modern unconsolidated aeolian layer to remain mostly intact.



Figure 33: Areas of high archaeological potential identified from analysis of the magnetometry survey.

6.3 Magnetic Susceptibility

All four magnetic sustainability tests produced similar results, despite being located within different parts of the site and ending at varying depths. The majority of the magnetic susceptibility in each trench maintains a similar value of roughly 0.5 to 1 SI and does not deviate very often.

The first of the anomalies detected is a small area of very high susceptibility located near the surface of each trench. Across three of the four tests, the first result measured 10 SI and higher, and in the only test where this was not the case, Trench 5, the reading was still significantly higher at the start compared to the rest of the trench. This anomaly has been identified as the metal bracket of the tape measure used to mark every 2 cm measurement, which was noted during fieldwork. Under this initial spike in magnetic susceptibility, every trench has a much smaller increase in susceptibility around the depth of 15 to 20 cm. This minor increase in magnetic susceptibility across the site is likely due to the formation of the topsoil. Another anomaly that occurs in all test results is a significant increase in magnetic susceptibility at the bottom of each trench. Trench 6 does not display a sudden increase as the other trenches do but still has a slight sustainability increase at the base of the pit. The fact that each trench ends at different depths makes it difficult to identify what this anomaly could be. It may be the beginning of a paleosol, however, it may also be an operator or machine error.

The final anomaly detected occurs in Trench 10 around the depth of 60 cm. Here there is a significant increase in susceptibility, which corresponds with an artefact layer that was identified at the same depth during the excavation of Trench 10. This

increase could thus be evidence of a paleosol within KH1. Interestingly, this anomaly only occurs within Trench 10, which was the only trench tested on the eastern side of the fence line, while the other trenches are on the western side.

The results of these magnetic susceptibility tests on trenches west of the fence line, Trenches 1, 5 and 6, have not identified any definite paleosols within the subsurface of KH1. However, this is understandable given that unlike Trench 10, no archaeological layer was identified during the excavation of these trenches. The size of the archaeological associated unit, the semi consolidated aeolian sediment, is also significant. As the ERT revealed, this unit spans six to eight metres deep, which means these trenches, with depths of 1.8 to 2.4 metres, are not significantly penetrating this unit. The fact that a paleosol has been identified east of the fence line, but not on the western side, is likely due to the minimal erosion that has occurred east of the fence. The magnetic susceptibility tests did reveal that if any paleosols are present on the western side of KH1, they must be deeper than 2 metres under the surface.

6.4 Summary

Archaeology

The potential hearth anomalies identified by the magnetometry survey are mostly concentrated in the northwest section of the survey area, close to the riverbank. This is likely due to the considerable erosion that has occurred in this area of KH1, causing deeper parts of the semi consolidated aeolian unit to be exposed. The correlation between the bifacial cluster and prehistoric burning means that these hearth anomalies are likely areas of high archaeological potential and where future

excavations of the site should consider focusing their efforts. However, the magnetic susceptibility data indicates that on the western side of the site there does are no definite paleosol within the first two metres of the subsurface. The two ERT lines on this side of the site demonstrate that the stratigraphic unit associated with the surface archaeology is up to eight metres in depth. Therefore, any future excavations on western KH1 will need to be prepared for potentially deep excavations, at least two metres deep and potentially up to eight metres under the surface.

This would be exacerbated on the eastern side of KH1 where the ERT revealed that the layer of modern semi consolidated sediment is thicker than originally thought. This unit pushed the archaeological associated unit deeper meaning in some areas it is up to 10 metres below the surface. Although, the single magnetic susceptibility test that was located on the eastern side of the fence line did reveal a potential paleosol within the subsurface. Thus, an excavation on this side of the site may only need to dig around 60cm deep to find archaeological material Although, it should be noted that no hearth anomalies were revealed east of the fence line, likely due to the thick layer of modern sediment and that this interpretation is only based off a single magnetic susceptibility test.

Depositional History

While the ERT did not reveal anything distinct about the archaeology of KH1 it did provide a much better understanding of the stratigraphy. The results identified that the surface of KH1 is made up of four distinct units, modern unconsolidated aeolian sediment, semi consolidated aeolian sediment, cobble sized fluvial sediment unit,

and highly resistive sediment deep in the subsurface which is likely bedrock. The top layer of the modern unconsolidated aeolian is generally less than a metre thick on the western side of the site, however, east of the fence line, this unit is consistently two metres thick and in parts of the site goes deeper. This can be contributed to the severe erosion that has taken place west of the fence, while the eastern side has been relatively protected. The archaeological associated unit, the semi consolidated aeolian sediment, was discovered to be significantly larger than originally thought and extends throughout the entirety of the site.

7 Conclusion

This chapter will summarise this research project and the key points of the geophysical survey. It will also discuss the limitations of the geophysical survey and consider the direction of future work at KH1.

7.1 The Geophysical Survey at KH1

This research project has demonstrated the benefit of geophysical techniques in studying open-air sites and has demonstrated what geophysical geoarchaeology can reveal about the archaeology and depositional history of an open-air site. The project has also outlined the effectiveness of each geophysical method in this survey and summarised how a multiple method approach is more beneficial than using a single technique.

While the ERT survey did not directly identify archaeological material, it did provide an improved understanding of the stratigraphy of KH1. The magnetometry data identified locations of high archaeological potential by locating subtle hearth anomalies within the surface that are associated with stone tools. Finally, the magnetic susceptibility tests revealed that on the western side of KH1 there does not seem to be a paleosol within the first two metres of the subsurface, but on the eastern side of the fence there is a potential paleosol 60cm under the surface. The results from these techniques combined have identified areas of archaeological potential and the likely depths of said archaeology, which a single method could not have done.

The results from the geophysical survey have established how important geophysical methods can be when surveying a large open-air site such as KH1, where

excavation can be expensive and time-consuming. A geophysical survey utilising multiple techniques can identify areas on an open-air site with high archaeological potential. By focusing excavations of these areas, the cost and time needed are substantially decreased and the likelihood of uncovering archaeology is increased. This project has also found that these geophysical methods work effectively in a southern African context.

7.2 Limitations

A limitation of the ERT survey conducted as part of this research project was the number of lines completed. While the results of the surveys provide a detailed snapshot of the subsurface of KH1 in three different areas, including how the subsurface differs on each side of the fence line, more lines would have been beneficial. Some additional north to south lines between the three conducted could have provided a better idea of how the subsurface changes over the site, especially between the eastern and western sections. East to west lines would also have been useful as they would have given a better idea of how the stratigraphy changes throughout the site, as well as complimenting the north to south lines already completed. An east to west line was planned for this geophysical survey, however, due to the harsh terrain of KH1, the ERT stopped working towards the end of the field session. The biggest problem with carrying out additional lines is the time required to do so. Each 64-metre section took 2-3 hours to set up and complete, resulting in only two or three 64-metres sections being accomplished each field day. Therefore, any additional line would have taken a substantial amount of extra time which was not available, and the extra data gained from these lines would not be significant to the project overall.

A major limitation regarding the magnetometry survey was the presence of modern metals on the surface and in the near-surface. The magnetometry survey area was examined for any modern metal, which was then removed from the area before any survey was conducted. However, it is evident in the magnetometry results that there was still modern metal present, at least within the near-surface. This is apparent by the high magnetic intensity anomalies in the results that are characteristic of ferrous metals. These magnetic anomalies are very common around the fence line, which provides a distinct feature within the survey results that can assist with interpretations. The problem with modern metals within the survey area is that the strong signal emitted by them can hide more subtle anomalies, such as those created by hearths which was the primary target of this magnetometry survey. However, even with a more thorough investigation of the survey area for modern metal, it is very unlikely that it could all have been found and removed from the survey area.

The largest limitation of the geophysical survey is ground proofing. At this time no further trenches or excavations have been conducted at KH1 which means many of the results of this research project are interpreted based on the geology, topography, and archaeology of the site. However, even with only inferences, the results of this project can still assist in future excavations and research at KH1. Even if the conclusions made by this project are proven inaccurate by future ground proofing, the results of a geophysical survey are not static and can be re-evaluated using new information in the future.

7.3 Future Research

Additional geophysical surveys at KH1 could be beneficial in gaining a better understanding of the subsurface there. As mentioned, more ERT lines across the site, especially in an east to west orientation, could provide a greater understanding of the stratigraphy of KH1. If enough extra lines were conducted, then a 3D model of the subsurface of KH1 could be created which would be more effective in interpreting and visualising the results compared to 2D models. While additional ERT lines would be valuable to understanding KH1, they are not necessary as the data gained from them would likely not be worth the time to perform the survey.

Expanding the magnetometry survey area north and west could identify further hearth anomalies within the subsurface. This is due to the eastern side of the current survey area having no identifiable hearth anomalies and the southern side containing very few of these anomalies as well as bordering the scree slope. Meanwhile, most of the subtle anomalies detected are within the northwest section of the survey area. The modern sediment unit is also less prominent in these areas compared to the western side and therefore additional grids in these directions could identify further hearths. These extra grids would also be very time-efficient, likely taking less than a day of fieldwork.

While eleven test trenches were dug during the field session, only four had magnetic susceptibility tests conducted on them. Additional magnetic susceptibility tests on the other seven trenches could provide more thorough data about the subsurface of KH1. Specifically, further tests on the other trenches east of the fence line would be important to identify if the anomaly found in Trench 10 is a paleosol is a continuous or isolated feature. Like the additional magnetometry grids, these subsequent tests would not take up much time.

As discussed, the lack of ground-truthing is a limitation of this project, which is why future test pits to ground proof the anomalies discovered would be beneficial. If the results from the test pits support the results of this research project, then it will validate the rest of the results. However, even if ground proofing refutes the interpretation of the geophysical surveys, then new interpretations can be made. In either case, ground proofing will provide a more accurate understanding of the subsurface at KH1 and is therefore highly recommended as a future pursuit.

This research project has verified that geophysical techniques are effective and beneficial to the study of open-air sites in a southern African context. The geophysical survey was conducted on KH1, however, the survey of other open-air sites in the region could be valuable. The results of this survey are a snapshot of the subsurface at KH1 which is likely similar to other open-air sites in the region. However, the geophysical survey of additional sites could further character the subsurface of the larger area rather than just KH1. These surveys could also provide valuable information for each site, such as the areas of archaeological potential as this research project has accomplished KH1.

References

Ames, C.J.H., M. Shaw, C.A. O'Driscoll and A. Mackay 2020a A multi-user mobile GIS solution for documenting large surface scatters: An example from the Doring River, South Africa. *Journal of Field Archaeology* 45(6):394–412.

Ames, C.J.H., S. Chambers, M. Shaw, N. Phillips, B.G. Jones and A. Mackay 2020b Evaluating erosional impacts on open-air archaeological sites along the Doring River, South Africa: Methods and implications for research prioritization. *Archaeological and Anthropological Sciences* 12(103):1–15.

Archer, W., C.M. Pop, P. Gunz and S.P. McPherron 2016 What is Still Bay? Human biogeography and bifacial point variability. *Journal of Human Evolution* 97:58–72.

Armstrong, B.J., S. Edwards-Baker, P. Penzo-Kajewski and A.I.R. Herries 2021 Ground-penetrating radar analysis of the Drimolen early Pleistocene fossil-bearing palaeocave, South Africa. *Archaeological Prospection* 2021:1–15.

Backwell, L.R., F. d'Errico, W.E. Banks, P. de la Peña, C. Sievers, D. Stratford, S.J. Lennox, M. Wojcieszak, E.M. Bordy, J. Bradfield and L. Wadley 2018 New excavations at Border Cave, KwaZulu-Natal, South Africa. *Journal of Field Archaeology* 43(6):417–436.

Barde-Cabusson, S., X. Bolós, D. Pedrazzi, R. Lovera, G. Serra, J. Martí and A. Casas 2013 Electrical resistivity tomography revealing the internal structure of monogenetic volcanoes. *Geophysical Research Letters* 40(11):2544–2549.

Bartington a *Operations Manual for Grad-601 Single Axis Magnetic Field Gradiometer System*. England: Bartington Instruments Ltd.

Bartington b *Operations Manual for MS3 Magnetic Susceptibility Meter*. England: Bartington Instruments Ltd.

Bartington c *Operations Manual for MS2 Magnetic Susceptibility System*. England: Bartington Instruments Ltd.

Bolger, A. 2010 *Geophysics*. Jaipur: Oxford Book Co.

Campana, S. 2009 Archaeological site detection and mapping: Some thoughts on differing scale of detail and archaeological 'non-visibility'. In S. Campana and S. Piro (eds), *Seeing the Unseen: Geophysics and Landscape Archaeology*, p.27–66. London: Taylor & Francis Group

Chambers, J.E., P.B. Wilkinson, S. Penn, P.I. Meldrum, O. Kuras, M.H. Loke and D.A. Gunn 2013 River terrace sand and gravel deposit reserve estimation using

three-dimensional electrical resistivity tomography for bedrock surface detection. *Journal of Applied Geophysics* 93:25–32.

Clark, A. 1996 *Seeing Beneath the Soil: Prospecting Methods in Archaeology*. London: B.T. Batsford Ltd.

Cozzolino, M., E. Di Giovanni, P. Mauriello, S. Piro and D. Zamuner 2018 *Geophysical Methods for Cultural Heritage Management*. Cham: Springer International Publishing.

Dalan, R.A. and S.K. Banerjee 1998 Solving archaeological problems using techniques of soil magnetism. *Geoarchaeology* 13(1):3–36.

Dietl, H., A.W. Kandel and N.J. Conard 2005 Middle Stone Age settlement and land use at the open-air sites of Geelbek and Anyskop, South Africa. *Journal of African Archaeology* 3(2):231–242.

Fassbinder, J.W.E. 2017 Magnetometry for archaeology. In A.S. Gilbert (ed.) *Encyclopedia of Geoarchaeology*, p.499–514. Encyclopedia of Earth Sciences Series. Dordrecht: Springer.

Fowler, K.D., H.J. Greenfield and L.O. van Schalkwyk 2004 The effects of burrowing activity on archaeological sites: Ndongondwane, South Africa. *Geoarchaeology* 19(5):441–470.

Fuchs, M., A.W. Kandel, N.J. Conard, S.J. Walker and P. Felix-Henningsen 2008 Geoarchaeological and chronostratigraphical investigations of open-air sites in the Geelbek Dunes, South Africa. *Geoarchaeology* 23(4):425–449.

Geotomo 2019 *Rapid 2-D Resistivity & IP Inversion using the Least-Squares Method*. Malaysia: Geotomo Software SDN BHD.

Grassi, S., G. Patti, P. Tiralongo, S. Imposa and D. Aprile 2021 Applied geophysics to support the cultural heritage safeguard: A quick and non-invasive method to evaluate the dynamic response of a great historical interest building. *Journal of Applied Geophysics* 189:1–11.

Hallinan E. and J. Parkington 2017 Stone Age landscape use in the Olifants River Valley, Clanwilliam, Western Cape, South Africa. *Azania: Archaeological Research in Africa* 52(3):324–372.

Herries, A.I.R. 2009 New approaches for integrating palaeomagnetic and mineral magnetic methods to answer archaeological and geological questions on Stone Age

sites. In A. Fairbairn, S. O'Connor and B. Marwick (eds), *New Directions in Archaeological Science*, pp.235–253. Terra Australis 28. Canberra: ANU E Press.

Herries, A.I.R. 2010 Multidimensional GIS modeling of magnetic mineralogy as a proxy for fire use and spatial patterning: Evidence from the Middle Stone Age bearing sea cave of Pinnacle Point 13B (Western Cape, South Africa). *Journal of Human Evolution* 59:306–320.

Herwanger, J., H Maurer, A.G. Green and J. Leckebusch 2000 3-D inversions of magnetic gradiometer data in archaeological prospecting: Possibilities and limitations. *Geophysics* 65(3):849–860.

Hossain, S., G. Kibria and S. Kan 2018 *Site Investigation using Resistivity Imaging*. London: Taylor & Francis Group.

Idris, M. 2019 Evaluation of GPS-RTK and total station for topographic survey and strategic decision in private companies. *KnE Engineering* 4(3):323–332.

Jacobs, Z., E.H. Hayes, R.G. Roberts, R.F. Galbraith and C.S. Henshilwood 2013 An improved OSL chronology for the Still Bay layers at Blombos Cave, South Africa: Further tests of single-grain dating procedures and a re-evaluation of the timing of

the Still Bay industry across southern Africa. *Journal of Archaeological Science* 40:579–594.

Jordanova, N., D. Jordanova, A. Mokreva, D. Ishlyamski and B. Georgieva 2019 Temporal changes in magnetic signal of burnt soils – A compelling three years pilot study. *Science of the Total Environment* 669:729–738.

Kandel, A.W. and N.J. Conard 2005 Production sequences of ostrich eggshell beads and settlement dynamics in the Geelbek Dunes of the Western Cape, South Africa. *Journal of Archaeological Science* 32:1711–1721.

Kandel, A.W. and N.J. Conard 2013 Stone Age economics and land use in the Geelbek Dunes. In A. Jerardino, A. Malan and D. Braun (eds), *The Archaeology of the West Coast of South Africa*, pp.24–49. Cambridge Monographs in African Archaeology 84. Oxford: Archaeopress.

Kyriacou, K., J.E. Parkington, M. Will, A.W. Kandel and N.J. Conard 2015 Middle and Later Stone Age shellfish exploitation strategies and coastal foraging at Hoedjiespunt and Lynch Point, Saldanha Bay, South Africa. *Journal of Scientific Archaeology* 57:197–206.

Lin, S.C., M.J. Douglass and A. Mackay 2016 Interpreting MIS3 artefact transport patterns in southern Africa using cortex ratios: An example from the Putslaagte Valley, Western Cape. *Southern Africa Archaeological Bulletin* 71(204):173–180.

Linford, N. 2006 The application of geophysical methods to archaeological prospection. *Reports on Progress in Physics* 69:2205–2257.

Linford, N.T and M.G. Canti 2001 Geophysical evidence for fire in antiquity: Preliminary results from an experimental study. *Archaeological Prospection* 8:211–225.

Lombard, M., L. Wadley and J. Deacon 2012 South African and Lesotho Stone Age Sequence updated (1). *The South African Archaeological Bulletin* 67(195):120–144.

Low, M., A. Mackay and N. Phillips 2017 Understanding Early Later Stone Age technology at a landscape-scale: Evidence from the open-air locality Uitspankraal 7 (UPK7) in the Western Cape, South Africa. *Azania: Archaeological Research in Africa* 52(3):373–406.

Low, M. and A. Mackay 2018 The organisation of Late Pleistocene Robberg blade technology in the Doring River Catchment, South Africa. *Journal of African Archaeology* 16:168–192.

Mackay, A., A. Sumner, Z. Jacobs, B. Marwick, K. Bluff and M. Shaw 2014
Putslaagte 1 (PL1), the Doring River, and the Later Middle Stone Age in Southern
Africa's Winter Rainfall Zone. *Quaternary International* 350:43–58.

Mackay A., E. Hallinan and T.E. Steele 2018 Provisioning Responses to
Environmental Change in South Africa's Winter Rainfall Zone: MIS 5-2. In E.
Robinson and F. Sellet (eds), *Lithic Technological Organization and
Paleoenvironmental Change*, pp.13–36. Studies in Human Ecology and Adaptation,
vol 9. Cham: Springer.

Magnavita, C. 2016 Contributions of archaeological geophysics to field research in
Sub-Saharan Africa: Past, present, future. *Azania: Archaeological Research in Africa*
51(1):115–141.

Maki, D., J.A. Homburg and S.D. Brosowske 2006 Thermally activated mineralogical
transformations in archaeological hearths: Inversion from maghemite gamma Fe₂O₄
phase to haematite alpha Fe₂O₄ form. *Archaeological Prospection* 13:207–227.

McClellan, R.G. and W.F. Kean 1993 Contributions of wood ash magnetism to
archaeomagnetic properties of fire pits and hearts. *Earth and Planetary Science
Letter* 119:387–394.

Miller, C.E., S.M. Mentzer, C. Berthold, P. Leach, B. Ligouis, C. Tribolo, J. Parkington and G. Porraz 2016 Site-formation processes at Elands Bay Cave, South Africa. *Southern African Humanities* 29:69–128.

Milsom, J. and A. Eriksen 2011 *Field Geophysics, Fourth Edition*. Chichester: John Wiley & Sons Ltd.

Moffat, I., J. Garnaut, C. Jordan, A. Vella, M. Bailey and Gunditj Mirring Traditional Owners Corporation 2016 ground penetrating radar investigations at the Lake Condah Mission Cemetery: locating unmarked graves in areas with extensive subsurface disturbance. *The Artefact* 39:8–14.

Papadimitrios, K.S., C. Bank, S.J. Walker and M. Chazan 2019 Palaeotopography of a Palaeolithic landscape at Bestwood 1, South Africa, from ground-penetrating radar and magnetometry. *South African Journal of Science* 115(1/2):1–7.

Papadopoulos, N.G., P. Tsourlos, G.N. Tsokas and A. Sarris 2006 Two-dimensional and three-dimensional resistivity imaging in archaeological site investigation. *Archaeological Prospection* 13:163–181.

Papadopoulos, N.G., A. Sarris, W.A. Parkinson, A. Gyucha, R.W. Yerkes, P.R. Duffy and P. Tsourlos 2014 Electrical resistivity tomography for the modelling of cultural deposits and geomorphological landscapes at Neolithic sites: A case study from Southeastern Hungary. *Archaeological Prospection* 21:169–183.

Phillips, N., J. Pargeter, M. Low, and A. Mackay 2019 Open-air preservation of miniaturised lithics: Experimental research in the Cederberg Mountains, southern Africa. *Archaeological and Anthropological Sciences* 11:5851–5877.

Piro, S. 2009 Introduction to Geophysics for Archaeology. In S. Campana and S. Piro (eds), *Seeing the Unseen: Geophysics and Landscape Archaeology*, p.27–66. London: Taylor & Francis Group.

Pollard, T., I. Banks, J. Arthur, J. Clark and N. Oliver 2013 Survey and excavation of the Anglo-Zulu War fort at Eshowe, KwaZulu-Natal, South Africa. *Journal of Conflict Archaeology* 1(1):133–180.

Porraz G., I. Marina, P. Schmidt and J.E. Parkington 2016 A shape to the microlithic Robberg from Elands Bay Cave (South Africa). *Southern Africa Humanities* 29:203–247.

Saad, R., M.N.M. Nawawi and E.T. Mohamad 2012 Groundwater detection in alluvium using 2-D electrical resistivity tomography (ERT). *Electronic Journal of Geotechnical Engineering* 17:369–376.

Samouëlian, A., I. Cousin, A. Tabbagh, A. Bruand and G. Richard 2005 Electrical resistivity survey in soil science: A review. *Soil and Tillage Research* 83:173–193.

Schmidt, A. 2007 Archaeology, magnetic methods. In D. Gubbins and E. Herrero-Bervera (eds), *Encyclopedia of Geomagnetism and Paleomagnetism*, p.32–31. Encyclopedia of Earth Sciences Series. New York: Springer.

Schmidt, A. 2013 *Earth Resistance for Archaeologists*. Plymouth: AltaMira Press.

Shaw, M., C. Ames, N. Phillips, S. Chambers, A. Dosseto, M. Douglas, R. Goble, Z. Jacobs, B.G. Jones, S. Lin, M. Low, J. McNeil, S. Nasoordeen, C. O'driscoll, R. Saktura, T. Sumner, S. Watson, M. Will and A. Mackay 2019 The Doring River Archaeology Project: Approaching the evolution of human land use patterns in the Western Cape, South Africa. *PaleoAnthropology* 2019: 400–422.

Simyrdanis, K., I. Moffat, N. Papadopoulos, J. Kowlessar and M. Bailey 2018 3D mapping of the submerged *Crowie* barge using electrical resistivity tomography. *International Journal of Geophysics* 2018(1):1–11.

Tite, M.S. and C. Mullins 1971 Enhancement of the magnetic susceptibility of soils on archaeological sites. *Archaeometry* 13(2):209–219.

Toushmalani, R. 2010 Application and limitation of geophysical techniques in archaeology. *Australian Journal of Basic and Applied Sciences* 6(12):6440–6449.

Wadley, L. 2015 Those marvellous millennia: The Middle Stone Age of Southern Africa. *Azania: Archaeological Research in Africa* 50(2):155–226.

Watson, S., M. Low, N. Phillips, C. O’Driscoll, M. Shaw, C. Ames, Z. Jacobs and A. Mackay 2020 Robberg material procurement and transport in the Doring River Catchment: Evidence from the open-air locality of Uitspankraal 9, Western Cape, South Africa. *Journal of African Archaeology* 18(2): 209–228.

Weston, D.G. 2002 Soil and susceptibility: Aspects of thermally induced magnetism within the dynamic pedological system. *Archaeological Prospection* 9:207–215.

Will, M., A. Mackay and N. Phillips 2015 Implications of Nubian-like core reduction systems in southern Africa for the identification of early modern human dispersals. *PLoS ONE* 10(6):1–21.

Will, M., J.E. Parkington, A.W. Kandel and N.J. Conard 2013 Coastal adaptations and the Middle Stone Age lithic assemblages from Hoedjiespunt 1 in the Western Cape, South Africa. *Journal of Human Evolution* 64:518–537.

Witten, A.J. 2006 *Handbook of Geophysics and Archaeology*. London: Equinox Publishing Ltd.